

Assessment of Select Climate Change Impacts
on U.S. National Security

Center for International Earth Science Information Network
(CIESIN)
Columbia University

Working Paper

July 1, 2008

Marc A. Levy¹, Bridget Anderson¹, Melanie Brickman¹, Chris Cromer¹, Brian Falk¹, Balazs Fekete², Pamela Green², Malanding Jaiteh¹, Richard Lammers², Valentina Mara¹, Kytt MacManus¹, Steve Metzler³, Maria Muñiz¹, Thomas Parris³, Randy Pullen¹, Catherine Thorkelson¹, Charles Vorosmarty², Wil Wollheim², Xiaoshi Xing¹, Greg Yetman¹

- 1) Center for International Earth Science Information Network (CIESIN), Columbia University
- 2) Water Systems Analysis Group, Complex Systems Research Center, Institute for the Study of Earth, Oceans, and Space, University of New Hampshire
- 3) ISciences, Ann Arbor, Michigan

Contact information:

Marc A. Levy
Deputy Director
CIESIN
PO Box 1000
61 Route 9W
Palisades, NY 10964
marc.levy@ciesin.columbia.edu
Tel: +1 845-365-8964
Fax: +1 845-365-8922

Acknowledgements

This research was funded by the U.S. National Intelligence Council as an input to a National Intelligence Assessment on climate change implications for U.S. National Security produced May 2008.. The results and conclusions presented here reflect solely the work of the authors.

Table of Contents

Executive Summary.....	p.	iii
Framework of the Study.....	p.	1
Module 1: Global Sea Level Rise.....	p.	2
Module 2: Aggregate Impacts of Temperature Change.....	p.	30
Module 3: Water Scarcity.....	p.	46

Executive Summary

This report examines climate change impacts to U.S. national security by quantifying select impacts globally at the national level and identifying countries that are both at high risk from projected climate change and possess risk factors associated with political instability.

Exposure to global sea-level rise risk exposure is quantified by identifying low-elevation coastal zones (LECZ), at 1, 3, 5, 7, 9, 10 and 12 meters of elevation. Countries with high risk factors for instability that also have the most people exposed to sea-level rise include China, Philippines, India, and Indonesia. Those with the greatest percentage of population so exposed include Philippines, Egypt, and Indonesia. Within these countries, Egypt has especially high rates of population growth within the LECZ.

Aggregate climate change vulnerability is quantified by using an index that takes into account both projected temperature change and adaptive capacity. For countries with high risk factors for instability, the most vulnerable countries are South Africa, Nepal, Morocco, Bangladesh, Tunisia, Paraguay, Yemen, Sudan and Côte d'Ivoire.

Water scarcity is examined by comparing numbers of people living under conditions of water in the present with three future scenarios – one in which the climate remains unchanged but population changes; one in which population changes but the climate remains static; and one in which both population and climate change. Countries with high risk factors for instability that are projected to have the biggest increases in water scarcity are Mozambique, Côte d'Ivoire, Nigeria, Iraq, Guatemala, Zimbabwe, Ethiopia, Somalia, China, Syria and Algeria.

Framework of the Study

This report seeks to characterize a set of potential impacts of climate change that are relevant to U.S. security interests, utilizing country-level and aggregations of such impacts. It does not represent a comprehensive assessment of U.S. security interests potentially affected by climate change, but rather derives insights from a few approaches to impact analysis featured in the Fourth Assessment of the Intergovernmental Panel on Climate Change (IPCC) and the published literature on climate impacts. In particular, it explores the potential impact of sea-level rise through delineation of low-elevation coastal zones; it explores the potential aggregate impacts of temperature change through application of the IPCC's synthetic vulnerability approach; and it explores water scarcity through application of a global water balance model.

These three aspects of climate impacts were chosen because data and published methods were available that permitted calculation of comparable national indicators for virtually all countries. They do not represent the full range of climate impacts that might affect national security interests.

The potential climate impacts related to U.S. security interests are characterized with respect to recent experience with political instability and with instability risk factors. This framework represents a simple device for organizing results, and does not constitute formal predictions of where security problems are most likely. Rather, it is useful input into any discussion or qualitative analysis of plausible security threats from climate change.

Instability risks were identified through three factors. Dangerous neighborhoods were characterized by to the number of neighboring country-years experiencing major armed conflict during the period 1992-2005. "Very dangerous" neighborhoods were those with values of 30 or more; "moderately dangerous" neighborhoods were those with values between 10 and 29. Crisis history was characterized as an index constructed by summing the Political Instability Task Force (PITF) magnitude scores for each major instability event over the past 15 years. Values 30 and higher were considered "extremely high," values 10-29 were considered "moderately high," and values 1-9 were considered "somewhat high." Low capacity countries were identified by using the World Bank Government Effectiveness measure. Values below 1 were considered "low capacity." Countries were designated as having multiple risk factors if they fell into at least two of the following categories: Extremely Dangerous Neighborhood, Extremely High Crisis History, Low-Capacity.

These risk categories are based on an implicit heuristic model in which stress associated with climate change impacts has the potential to exacerbate security risks that may already be present in a country. They do not constitute a formal projection of where future security risks will be highest, or where climate change will generate new security problems.

Module 1: Global Sea Level Rise

To date, natural disaster hotspots are disproportionately located in low-lying coastal areas¹. Climate change is projected to increase coastal risks, including seaside erosion, sea-level rise and flooding due to increased storms. Additionally, coastal areas are becoming increasingly urban and this human development puts pressure on coastal areas, exacerbating coastal ecosystem damage². Therefore, it is useful to understand the distribution of population in low-lying coastal areas to the extent that they will be affected by seaward hazards due to coastal effects of climate change – inundation due to sea-level rise, stronger, more frequent storms with flood zones extending further inland, and displaced populations due to storm damages. In turn, it is useful to understand the distribution of population, and more specifically dense, urban population, to the extent it may exacerbate damages due to these seaward hazards. The physical infrastructure characteristic to urban development is costly to maintain and modify and would require relatively long lead times to relocate. Capacity constraints in resource-poor countries increase the challenge to adapt to coastal changes and hazards³. Thus, understanding the extent of risk to coastal populations, and, more specifically, urban cities can help to identify the best options for coping strategies, whether mitigation, modification, or migration⁴.

Urban, rural and total population were estimated by country for low elevation coastal zones of 1, 3, 5, 7, 9, 10 and 12 meters. These statistics were generated by overlaying a series of recently developed geographic datasets and performing zonal statistics to calculate the total value of each variable within each defined zone.

Data Sources

- 1) Land area: Global Rural-Urban Mapping Project (GRUMP) alpha.
<http://sedac.ciesin.columbia.edu/gpw/index.jsp>

The land area data used in this analysis come from the datasets developed in GRUMP alpha. Data include the geographic extent of each country and corresponding land area. These data come from a variety of sources including country statistical offices, UN agencies, and NGO's. Country borders are aligned (any mismatches rectified) and the data are converted into 30 arc-second resolution raster grids.

- 2) Urban Extents: Global Rural-Urban Mapping Project (GRUMP) alpha.
<http://sedac.ciesin.columbia.edu/gpw/index.jsp>

¹ Dille, Maxx, Robert S Chen, Uwe Deichmann, Arthur L Lerner-Lam and Margaret Arnold (2005), Natural Disaster Hotspots: A Global Risk Analysis, World Bank, Washington DC.

² IPCC. Working Group II Contribution to the Intergovernmental Panel on Climate Change Fourth Assessment Report Climate Change 2007: Climate Change Impacts, Adaptation and Vulnerability

³ IPCC. Working Group II Contribution to the Intergovernmental Panel on Climate Change Fourth Assessment Report Climate Change 2007: Climate Change Impacts, Adaptation and Vulnerability

⁴ McGranahan, G., D. Balk and B. Anderson. 2007. The rising tide: assessing the risks of climate change and human settlements in low elevation coastal zones. *Environment & Urbanization* 19(1). International Institute for Environment and Development (IIED).

Urban Extents data used in this analysis come from the datasets developed in GRUMP alpha. The urban extents are primarily derived from the DMSP 1994-1995 night-time lights dataset created by NOAA (<http://www.ngdc.noaa.gov/dmsp/download.html>) coupled with settlement information (e.g. name and population) to verify that the light corresponded to a human settlement. Urban and rural portions of the land area for each country's geographic extent are delineated in an urban-rural mask, a raster grid of 30 arc-second resolution, where 1 = rural and 2 = urban.

3) Population: Global Rural-Urban Mapping Project (GRUMP) alpha
<http://sedac.ciesin.columbia.edu/gpw/index.jsp>

The population data used in this analysis come from the datasets developed in GRUMP alpha. Data include population data for census units and settlements for each country. These data are attributed to subnational geographic boundaries and urban area locations to illustrate population distribution across a country. These data for each country have been converted into 30 arc-second resolution raster grids.

4) Elevation

ISciences produced a global set of Low-Elevation Coastal Zone delineations, at 3 arc-second resolution, using a variety of data inputs:

CGIAR

(<http://srtm.csi.cgiar.org/>)

The primary dataset for the elevation data below 60 degrees North was the CGIAR SRTM 90 meter version 3 dataset. This dataset is built in turn from the USGS DTED Level 1, which is the finished SRTM 3 product. CGIAR has enhanced the SRTM 3 by filling in voids within the data, masking off the ocean (which is set to 0 meters in the USGS dataset), and applying a hydrological flow enforcement algorithm.

USGS DTED Level 1

(<http://edcsns17.cr.usgs.gov/srtmdted/>)

A second source of elevation data below 60 degrees north was the USGS DTED Level 1 dataset (SRTM 3). Note that this dataset is what forms the basis for the CGIAR dataset listed above. It was used to fill in areas where the CGIAR dataset had dropped good SRTM data.

ISciences SRTM30

(<http://www.terraviva.net/srtm/index.html#SRTM30%20Global%20Elevation%20Enhanced%20-%20Slope/Aspect:>)

This data set was used for the area above 60 degrees North, and for the few areas below 60 degrees North where SRTM data wasn't available.

5) Watermask

USGS SRTM Water bodies Dataset

(<http://edc.usgs.gov/products/elevation/swbd.html>)

This is a set of shapefiles at 1 arc-second resolution that show where data within the USGS DTED dataset has been set to a fixed value. These were the primary source for the water mask used, although extensive editing of shapes within some 1 degree tiles was needed to correct for voids.

MDA Federal GeoCover

(<http://www.mdafederal.com/geocover/geocoverlc/>)

This is a 1 arc-second landcover dataset derived from LandSat images. Coverage is somewhat less than the SRTM dataset, but where this data existed it was the primary source for editing the USGS Water bodies.

Methodology

Development of the low elevation coastal zones:

The low elevation coastal zones (LECZs) were created using digital elevation model (DEM) data and a vector coastline layer. Zones of 1, 3, 5, 7, 9, 10, and 12 meters were delineated. LECZs were comprised only of grid cells that were contiguous with the coastline. Inland low-lying areas (less than or equal to 10(5) meters) that were not connected to the coast by adjacent low elevation land were excluded. The resulting dataset was converted into a raster mask, where 1 = low elevation coastal zone and all other land = no data.

Calculation of population and land area estimates

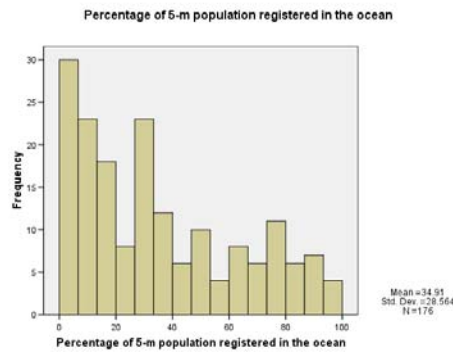
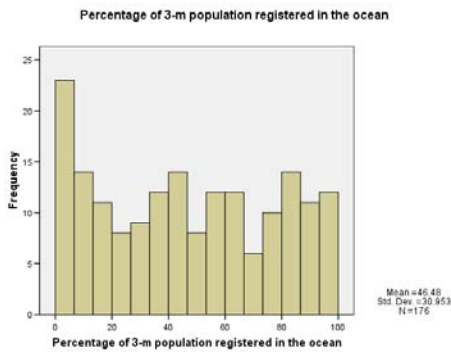
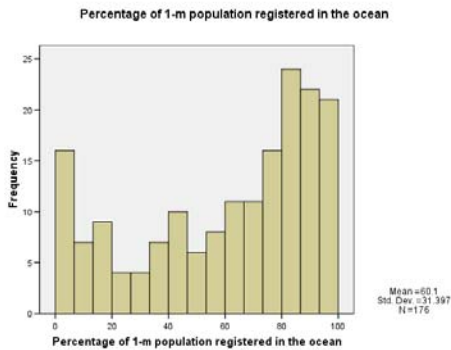
The population, land area and GDP estimates were generated through zonal statistics. All datasets had a matching resolution of 3 arc-seconds and a geographic projection and wgs84 datum. Therefore, by simply overlaying a geographic zone grid on a variable (population or land area grid, the sum of the data in the grid cells of the variable grid that overlap with the grid cells in the zone can be calculated.

Results

The results of this analysis should be seen as broadly indicative of relative exposure to sea-level rise risk, rather than precise predictions of numbers of people affected. Our ability to generate precise predictions is limited by the underlying accuracy of the elevation data, the spatial precision of the demographic data, an inability to know when sea level might hit certain benchmark levels, and the fact that although we assume a geographically fixed population to calculate exposure in reality highly affected regions will probably see out-migration.

The imprecision is greatest for the lowest-elevation zone. Prior work along these lines has tended to use higher elevation benchmarks for this reason. One way to quantify the amount of imprecision is to look at the number of people that our spatial databases locate, when overlaid with the elevation data, in the ocean. In reality, either the elevation data are inaccurate or the spatial population data is inaccurate. For our purposes we assumed that such people were in a coastal zone, and we include them in each coastal zone calculation. The percentage of a coastal zone's population that consists of people whose

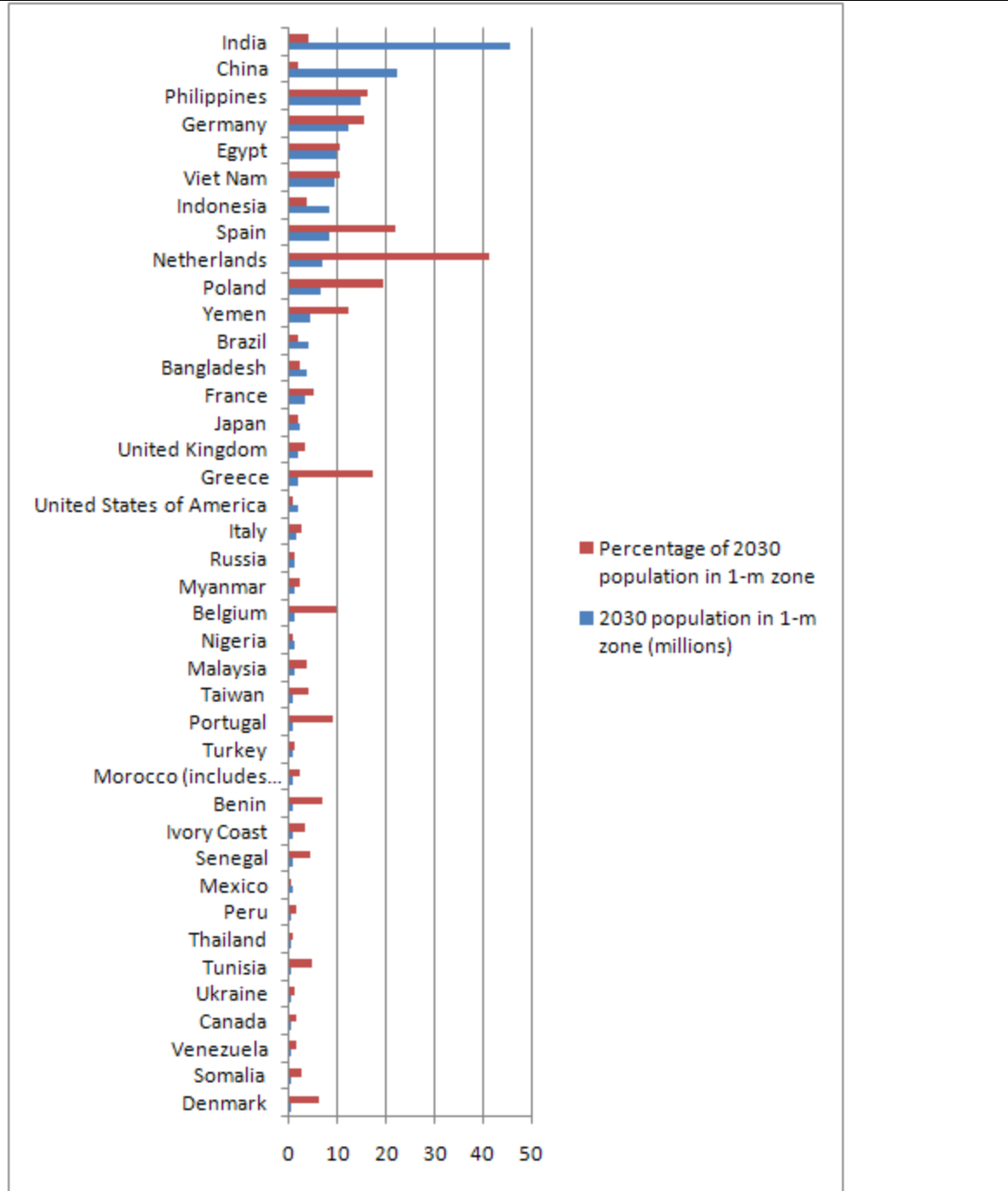
precise location is not really known is highest in the 1-m zone, as seen in this sequence of histograms.



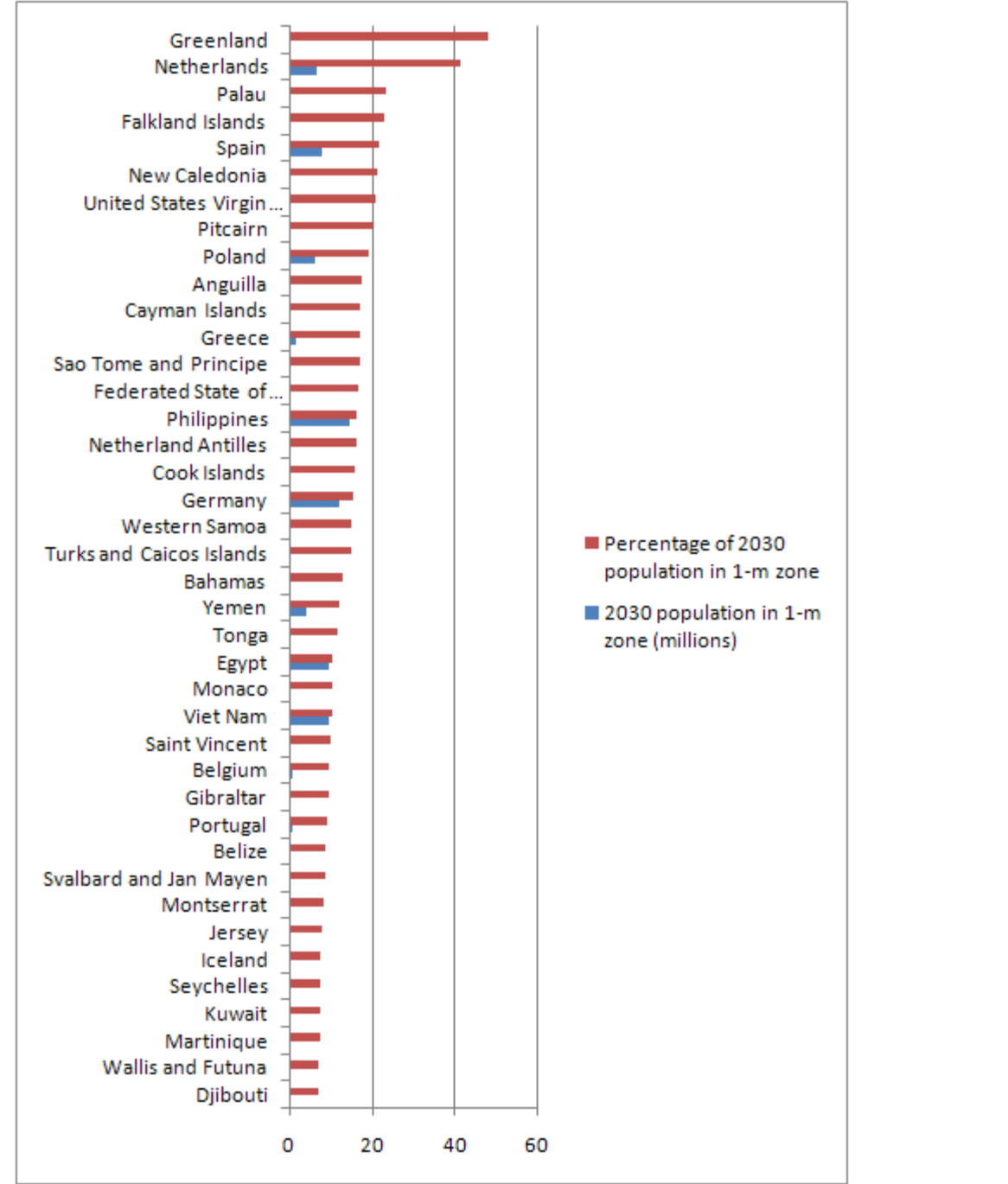
These different estimates are broadly correlated, and therefore the imprecision of the 1-meter estimates are not debilitating. The following scatterplot compares the 1-meter and 5-meter zones, in terms of percentage of population affected. Countries with very different values are highlighted. Some of these are probably different because of measurement error, while Viet Nam’s difference is consistent with earlier work we did comparing 5 and 10 meter zones – the concentration of people along the coast and hilly terrain make these numbers more plausible.

For country-specific analysis, the percentage of the country mis-located in the ocean, along with the local terrain and expert judgment, should be consulted to determine the magnitude of the possible measurement error.

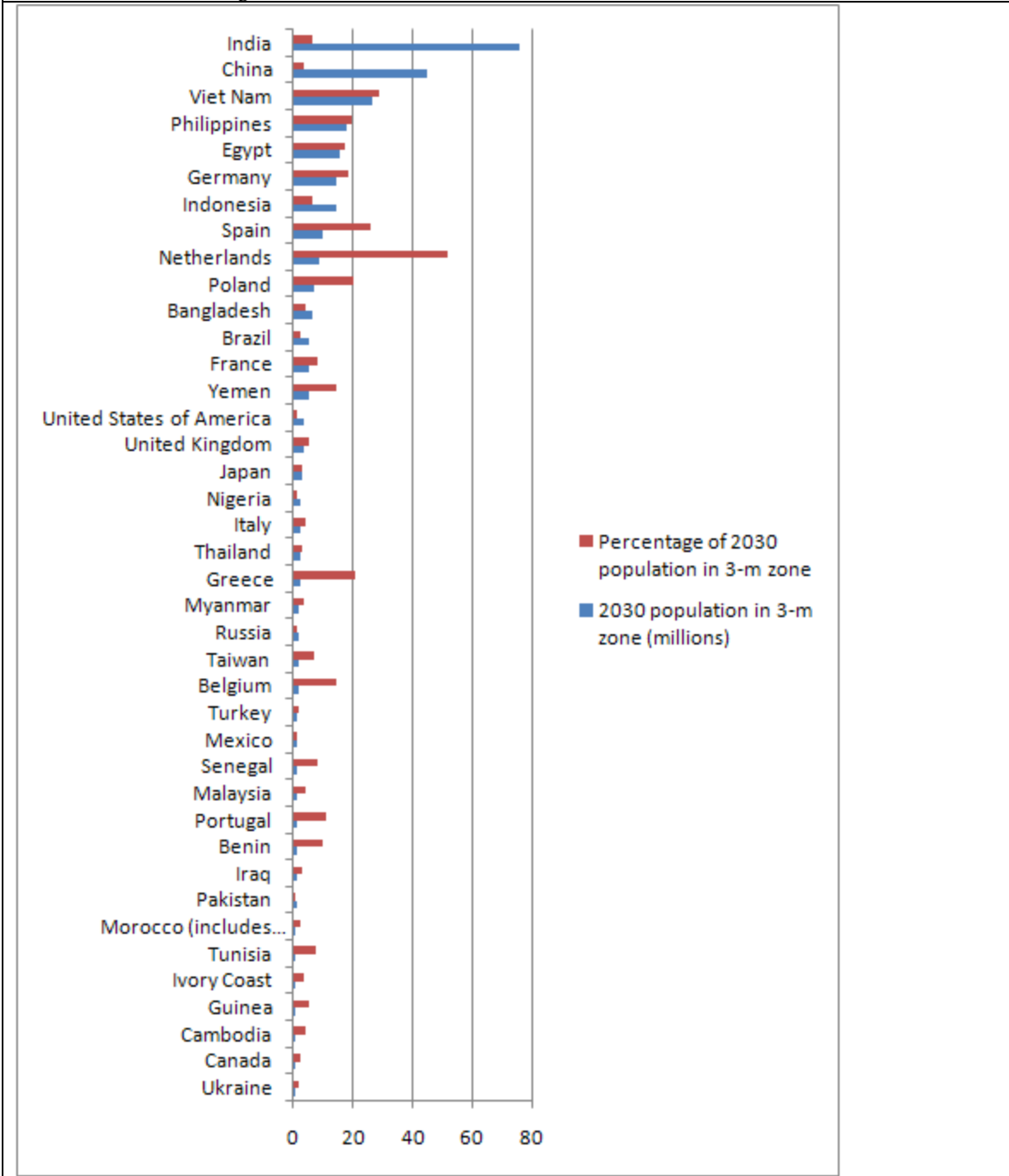
Countries with Greatest Total Number of People in 1-m Low-Elevation Coastal Zone, 2030.



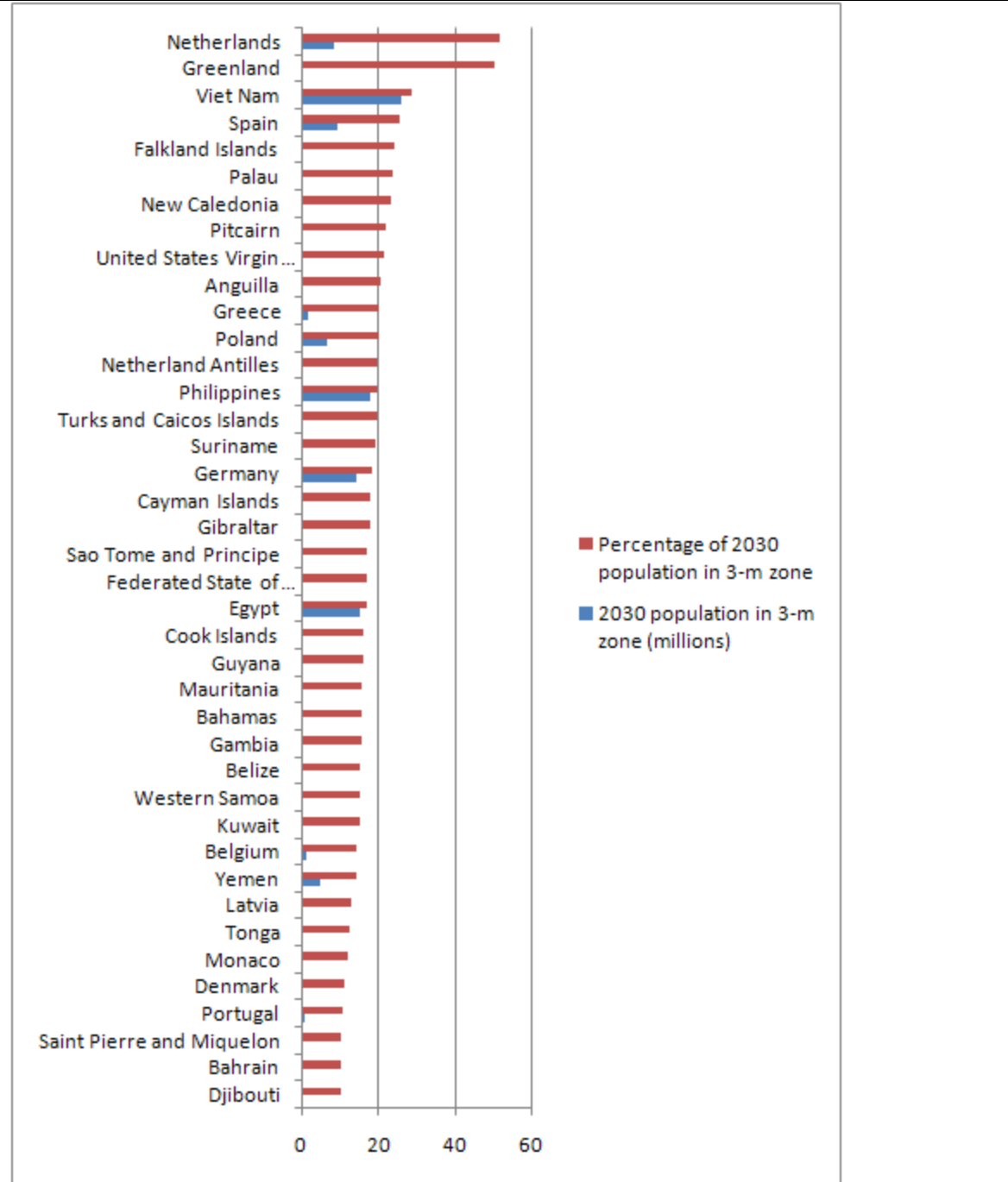
Countries with Greatest Percentage of National Population in 1-m Low-Elevation Coastal Zone, 2030.



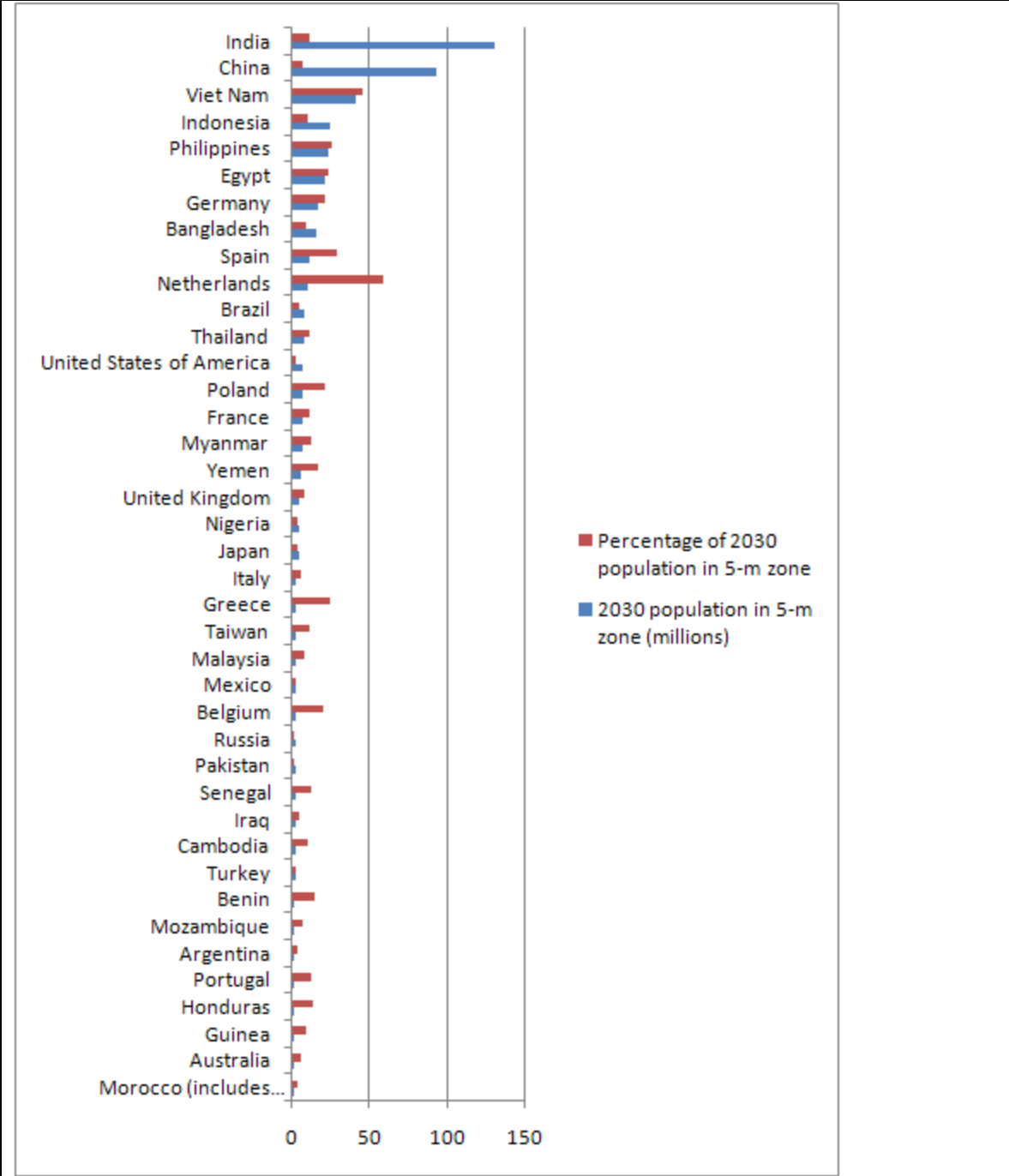
Countries with Greatest Total Number of People in 3-m Low-Elevation Coastal Zone, 2030 (sorted in descending order).



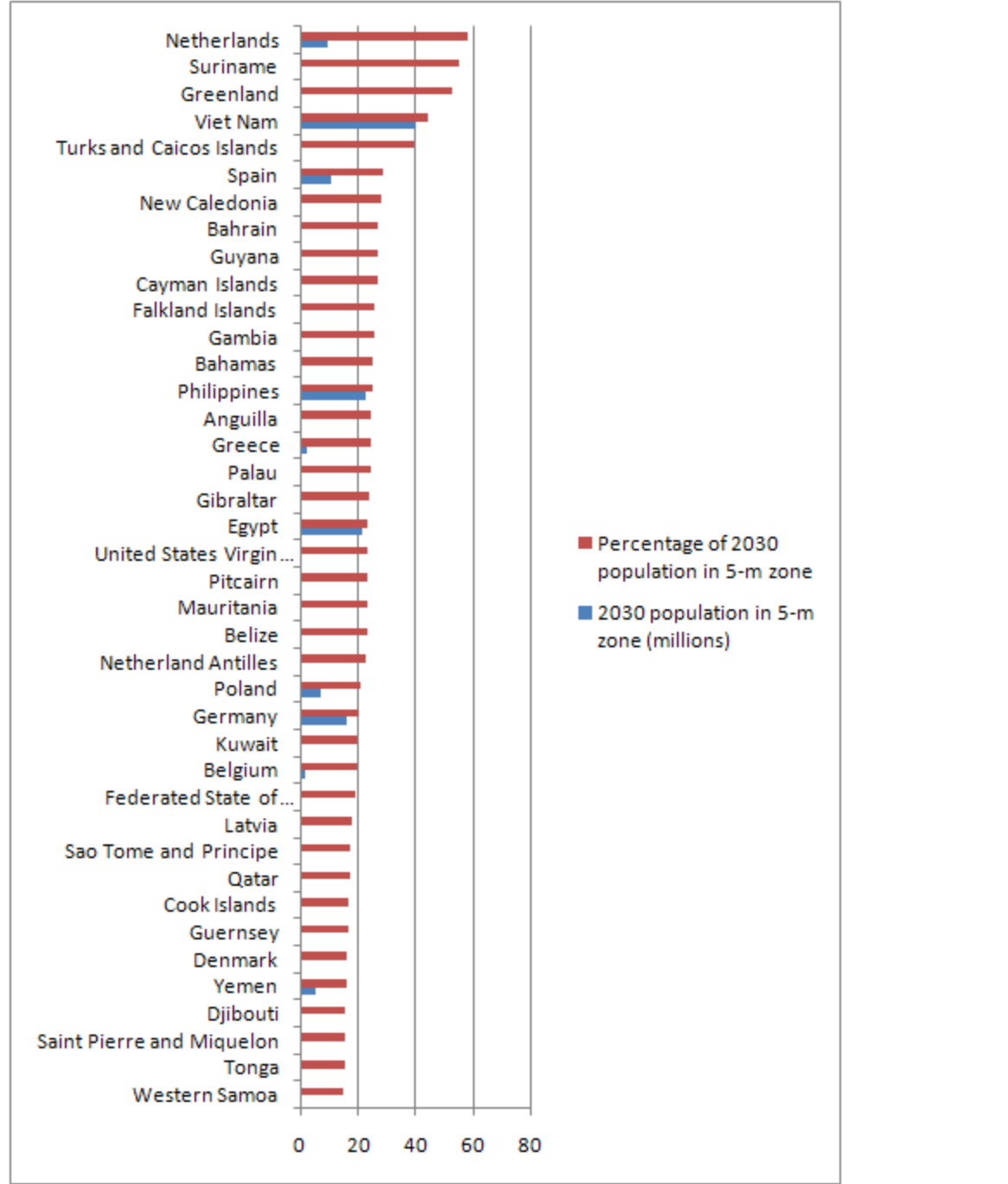
Countries with Greatest Percentage of National Population in 3-m Low-Elevation Coastal Zone, 2030.



Countries with Greatest Total Number of People in 5-m Low-Elevation Coastal Zone, 2030 (sorted in descending order).



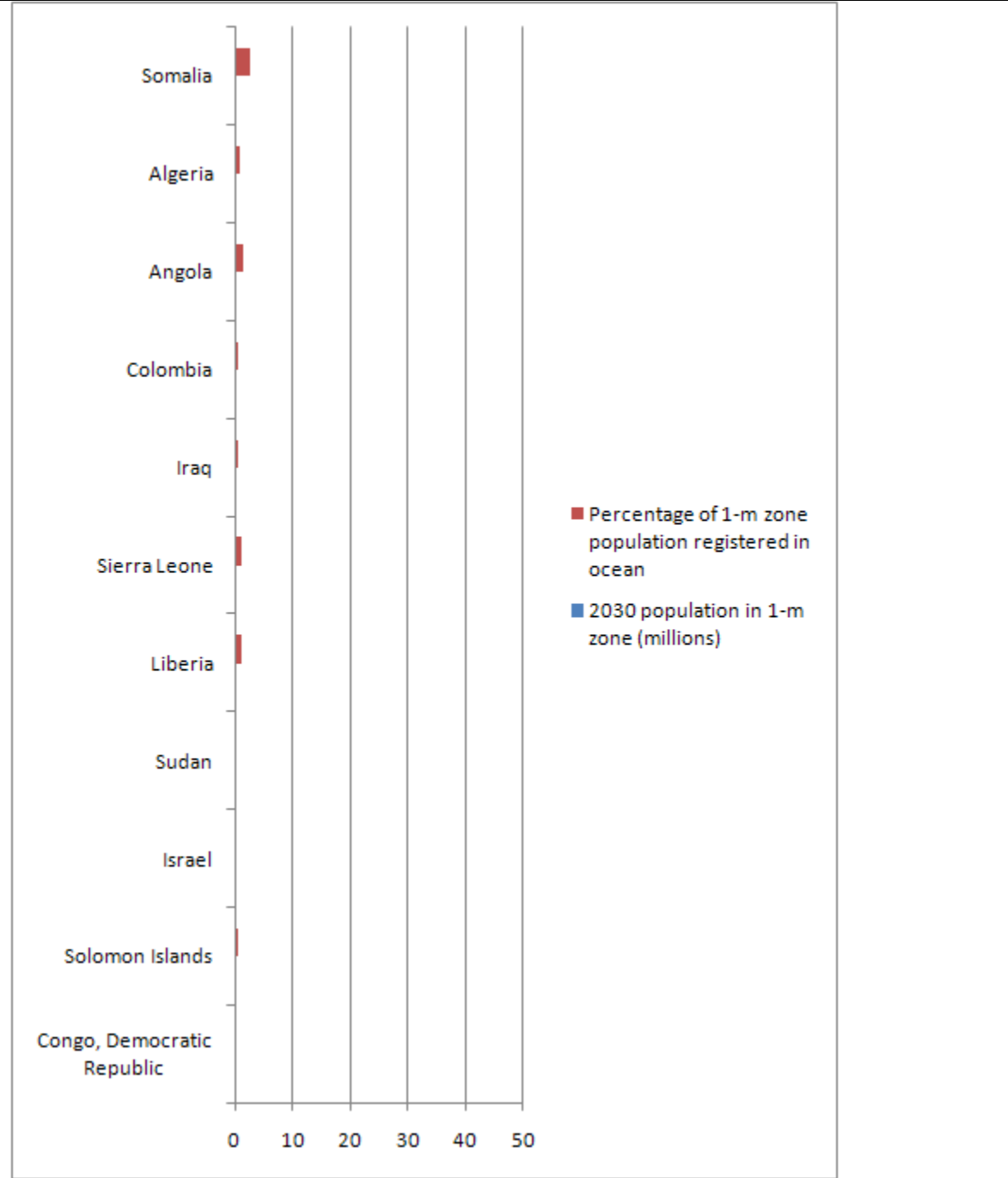
Countries with Greatest Percentage of National Population in 5-m Low-Elevation Coastal Zone, 2030.



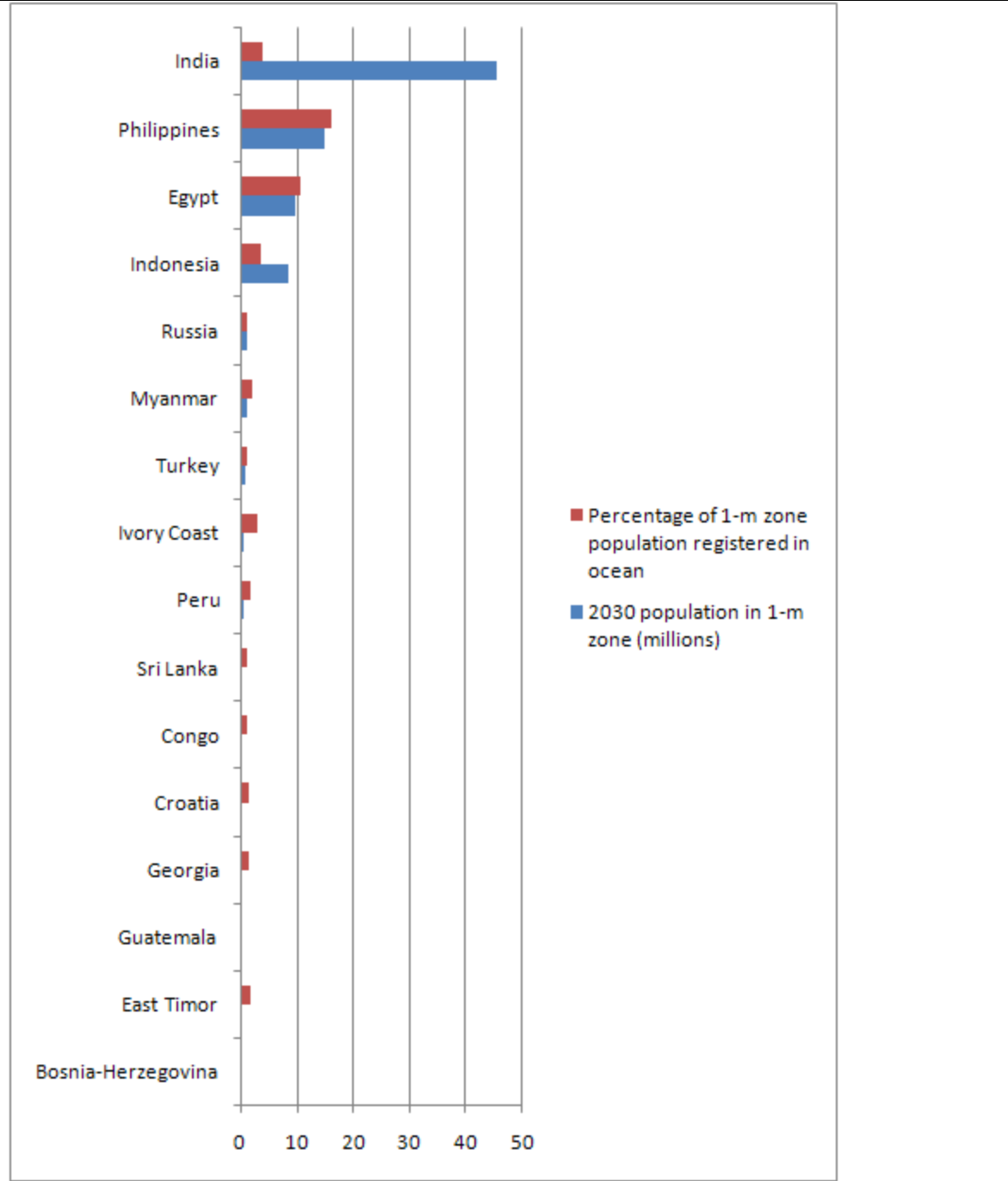
Countries with Two or More Instability Risk Factors (Dangerous Neighborhood, Crisis History, Low Capacity), sorted by Population in 1-m LECZ, 2030.



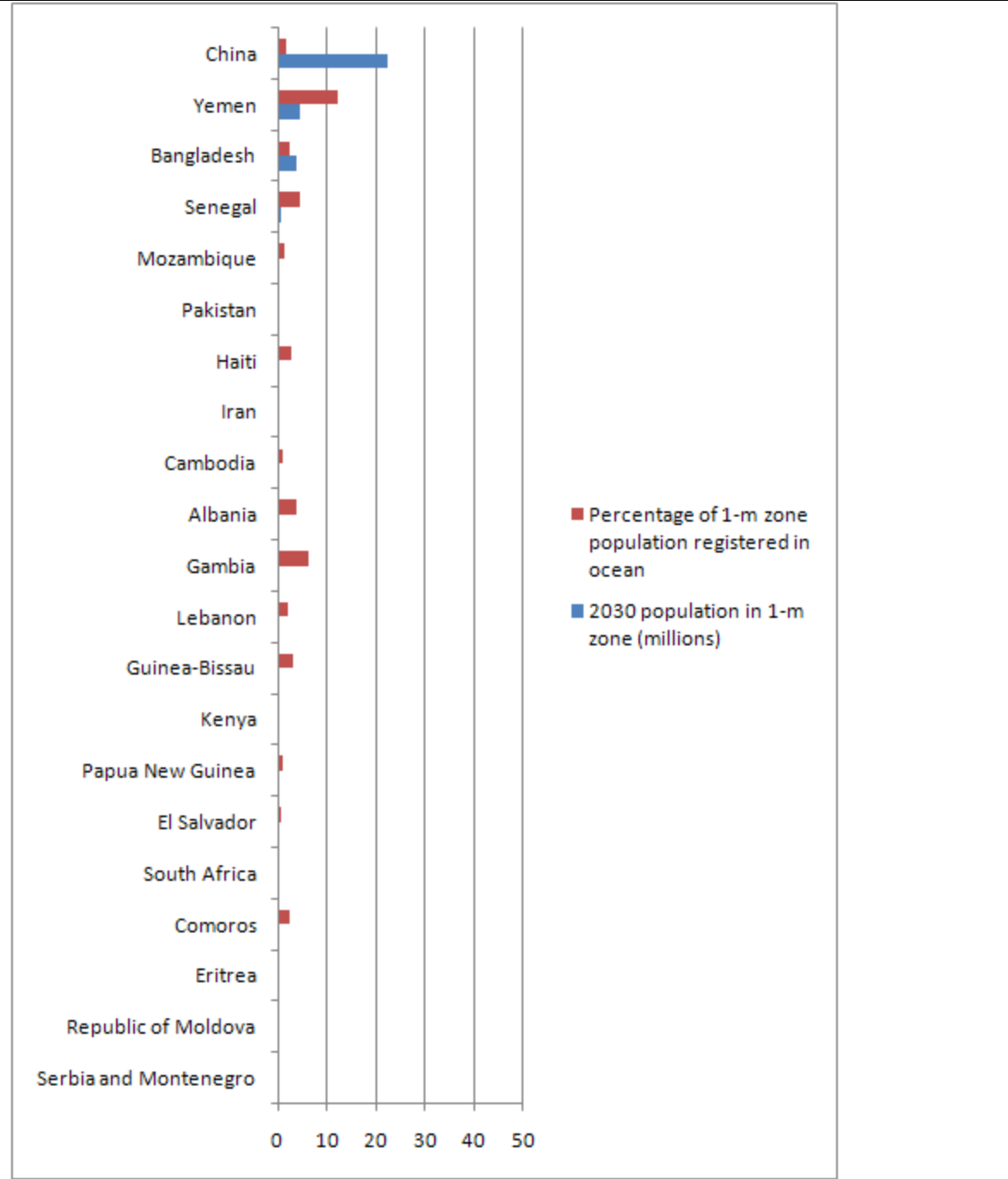
Countries with Extremely High Crisis History 1990-2005 (Sorted by population in 1-m LECZ, 2030)



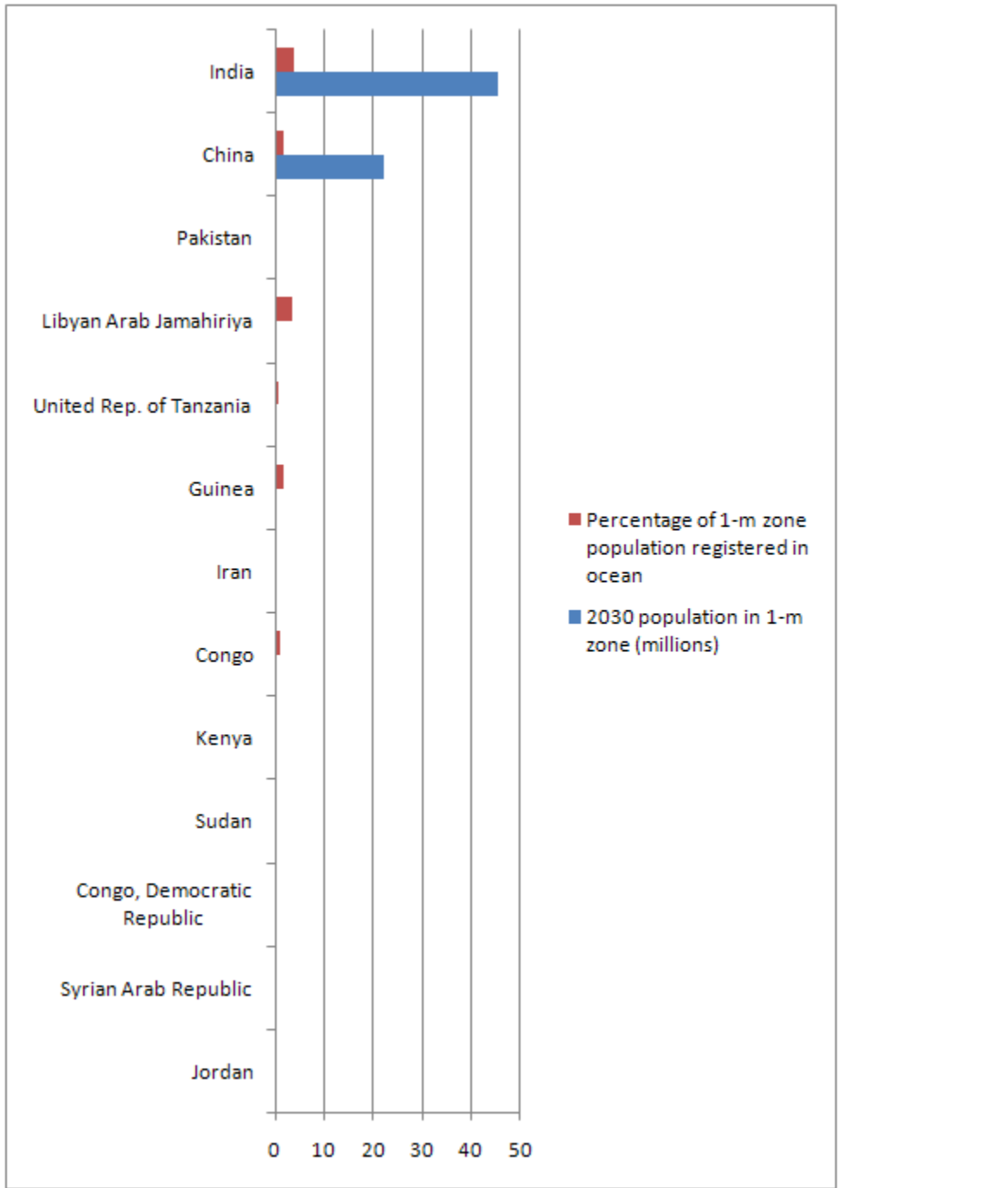
Countries with Moderately High Crisis History 1990-2005 (Sorted by population in 1-m LECZ, 2030)



Countries with Somewhat High Crisis History 1990-2005 (Sorted by population in 1-m LECZ, 2030)



Countries in Extremely Dangerous Neighborhoods (Sorted by population in 1-m LECZ, 2030)

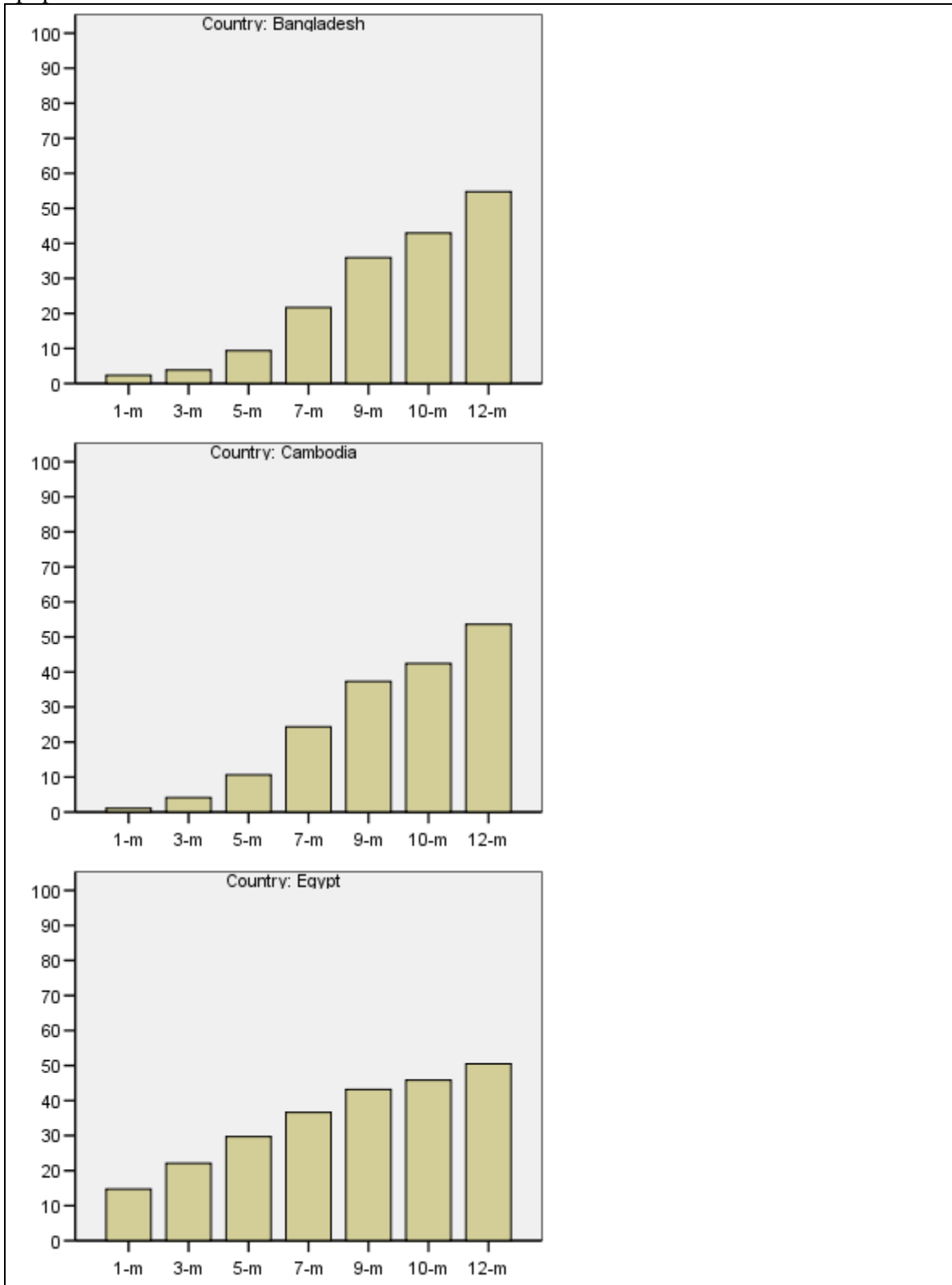


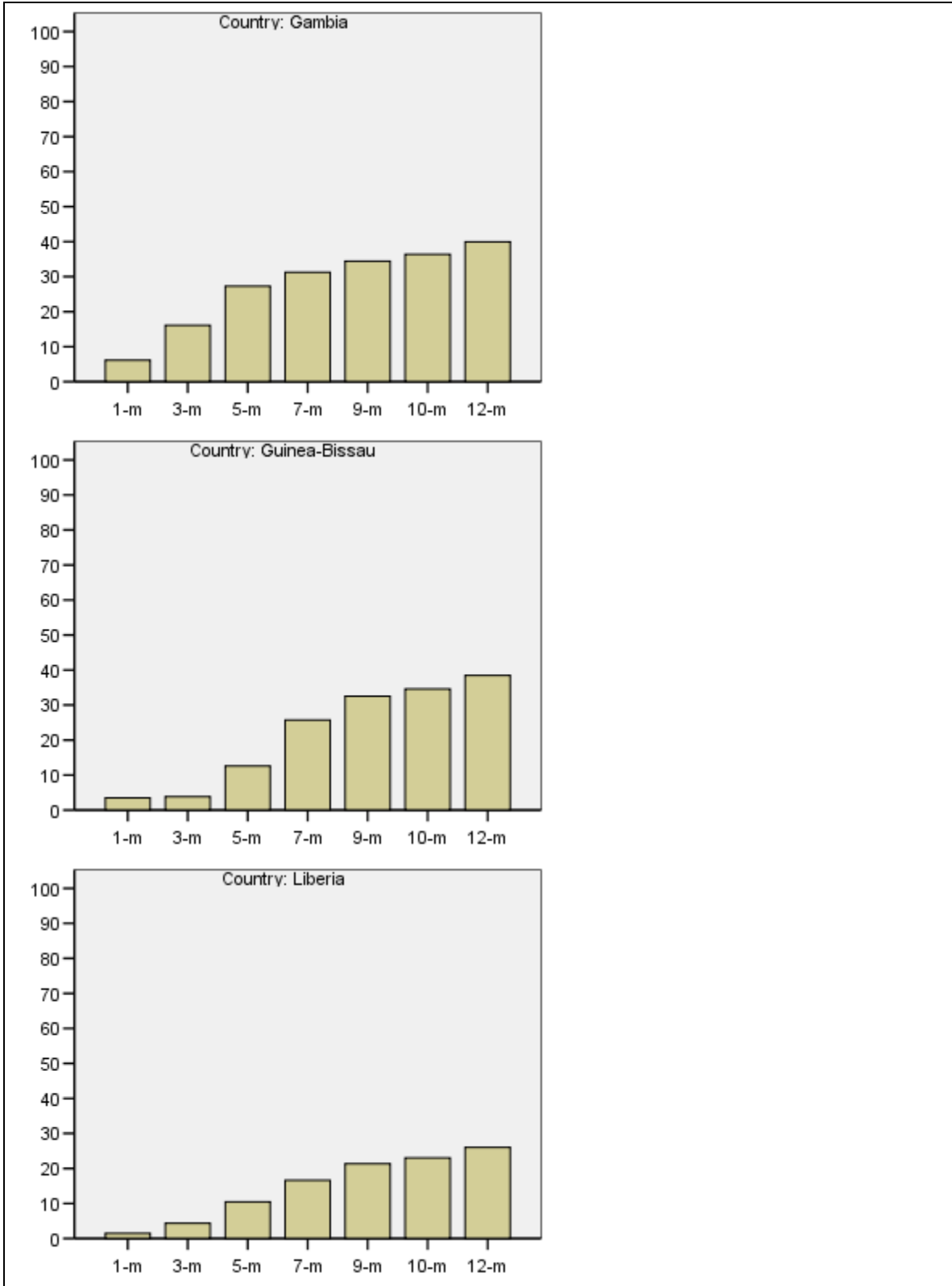
Countries in Moderately Dangerous Neighborhoods (Sorted by population in 1-m LECZ, 2030). Top 40 only.

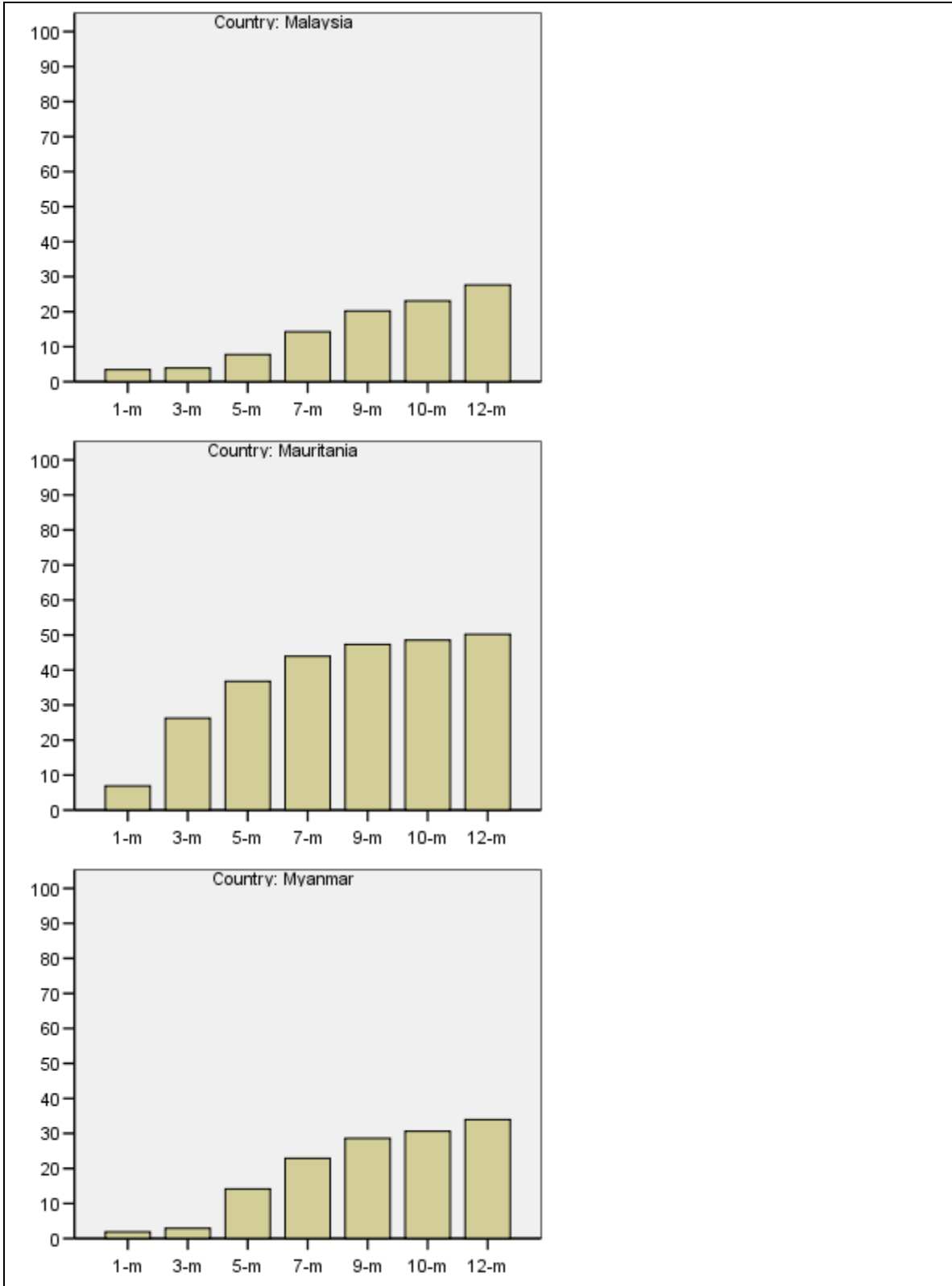


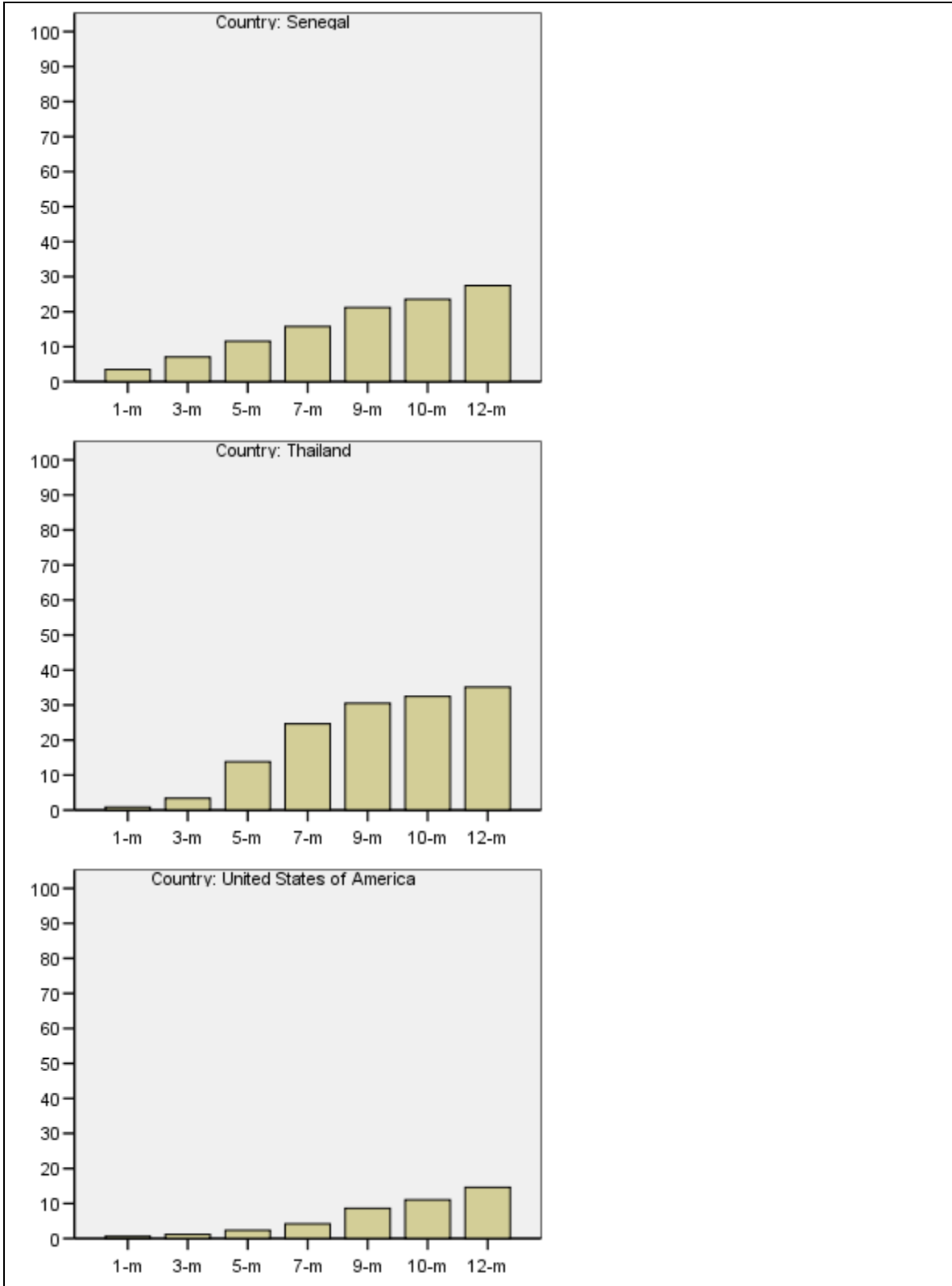


The following countries show the greatest variation across elevation zones, and would potentially benefit most from investment in improved elevation and georeferenced population data.



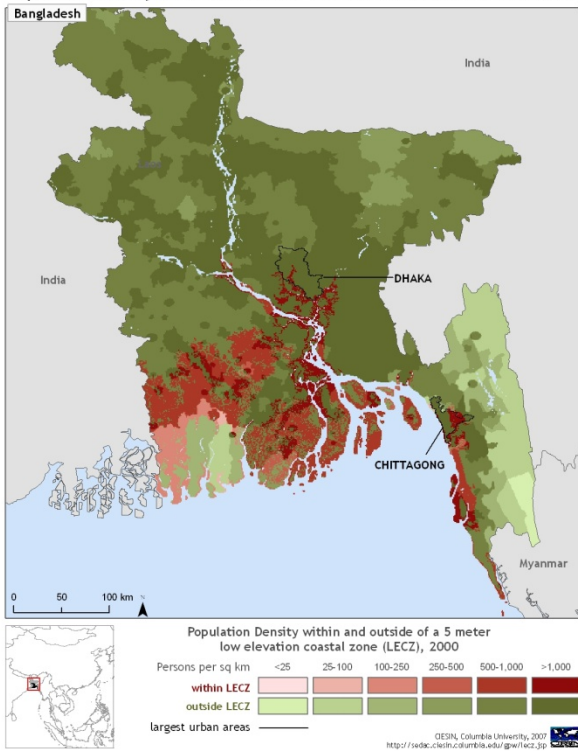




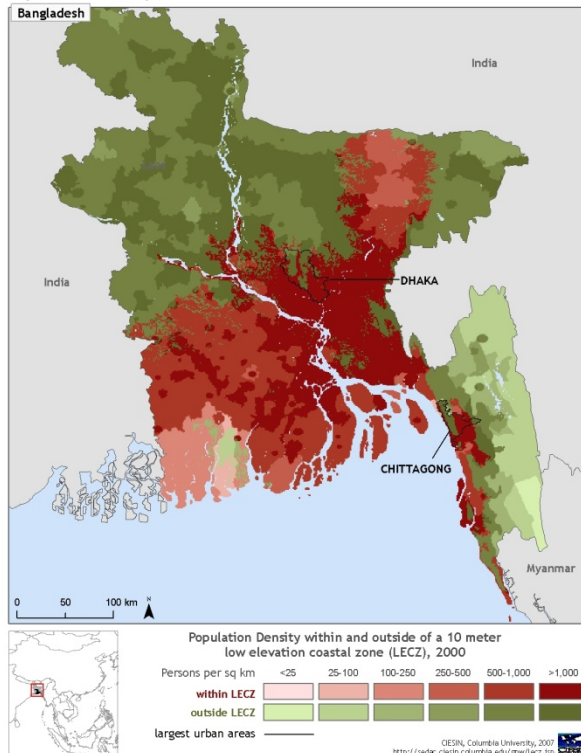


The following maps and calculations were produced using a preliminary version of the analysis based on coarser elevation data (1-km resolution). The broad visual patterns are similar to the later analysis though the numerical results differ slightly.

Population Density within and outside of a 5m Low Elevation Coastal Zone

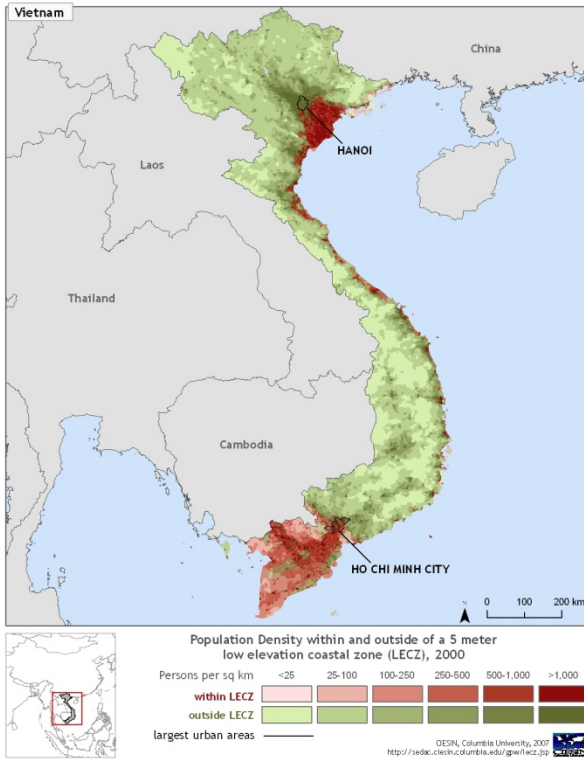


Population Density within and outside of a 10m Low Elevation Coastal Zone

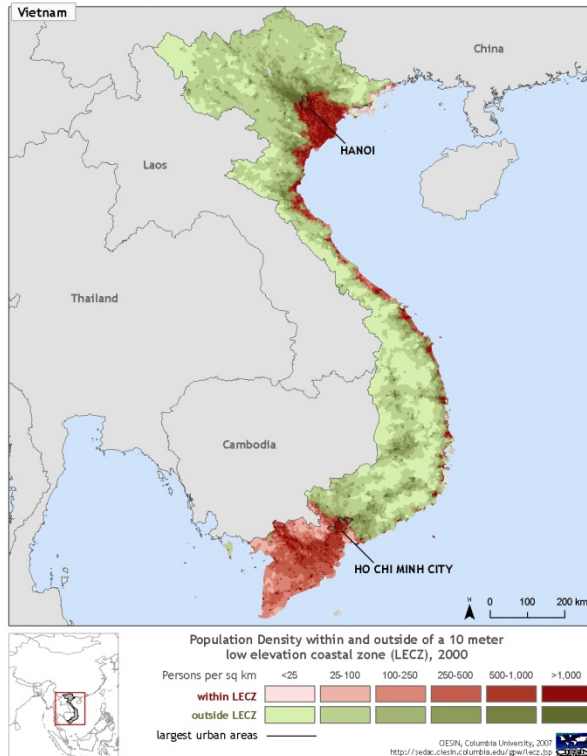


Bangladesh's history of recurrent flooding has led its residents to favor higher ground. As a result, far fewer people live within the 5-meter LECZ (11% of the population) than the 10-meter (46%). The percentage within the 10-meter is quite high by global norms.

Population Density within and outside of a 5m Low Elevation Coastal Zone

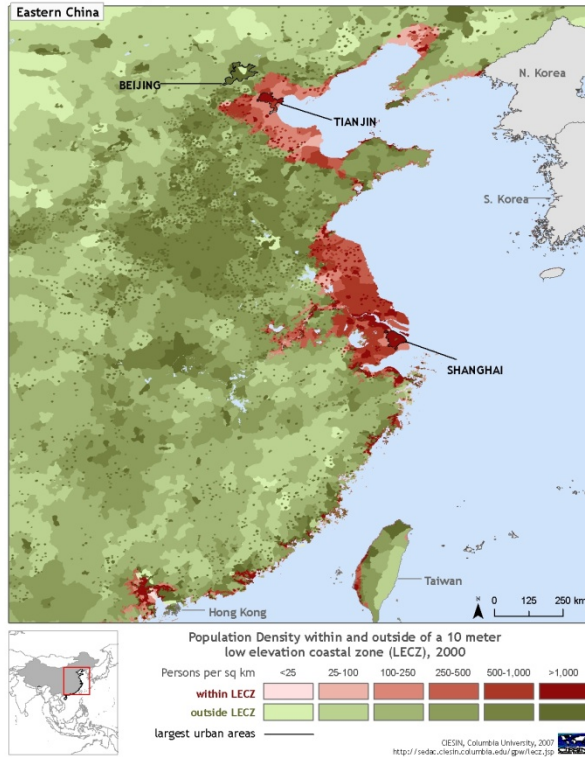


Population Density within and outside of a 10m Low Elevation Coastal Zone



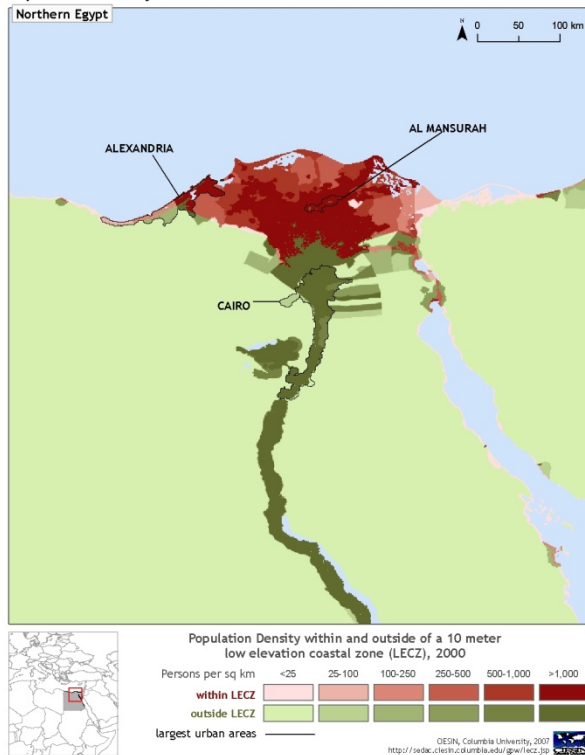
In Vietnam there is a very strong affinity between population and the coastal regions. As a result there is not much difference in the percentage of population living within the 10-meter LECZ (55%) and the 5-meter LECZ (39%). As a consequence, Vietnam is more sensitive to low levels of sea-level rise and associate coastal hazards than countries for whom the difference is greater.

Population Density within and outside of a 10m Low Elevation Coastal Zone



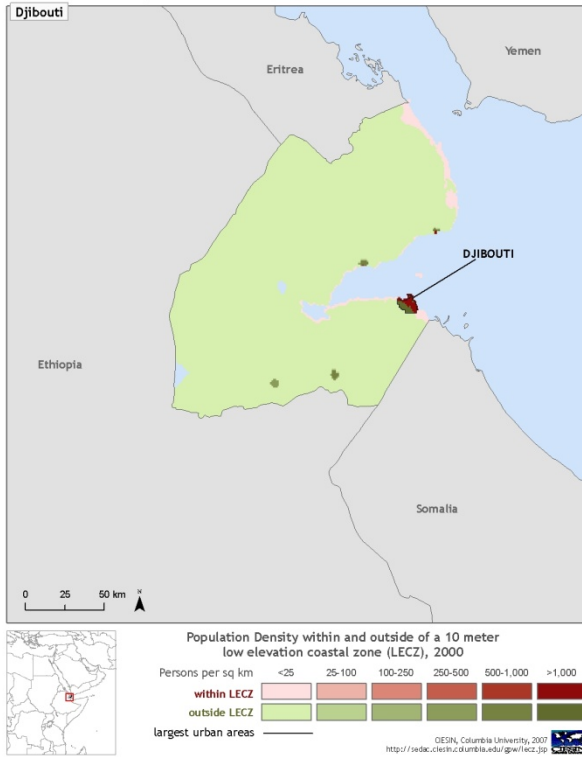
China has less exposure than Vietnam or Bangladesh within the 10-meter LECZ as a percentage of its total population (11%), but a large number of total people within the zone – 144 million. Because urban areas have an affinity for coasts, a larger percentage (18%) of China’s urban residents are within the 10-meter LECZ. And because coastal areas generate more economic activity, the 10-meter LECZ contains 35% of China’s urban GDP.

Population Density within and outside of a 10m Low Elevation Coastal Zone



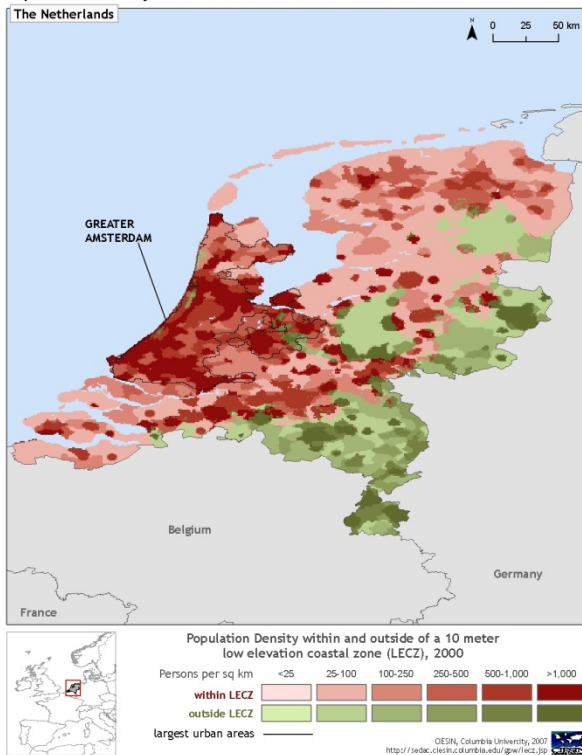
In Egypt population is highly concentrated along the Nile basin, whose delta is highly exposed to sea-level rise risk. A total of 37% of the country’s population lies within the 10-meter LECZ.

Population Density within and outside of a 10m Low Elevation Coastal Zone

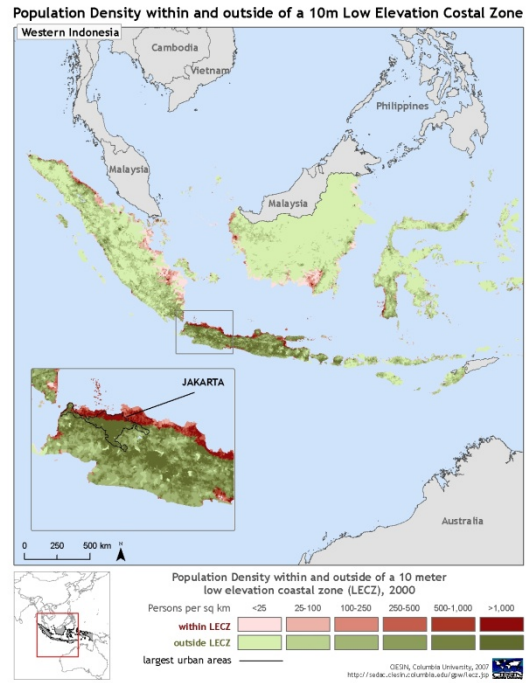
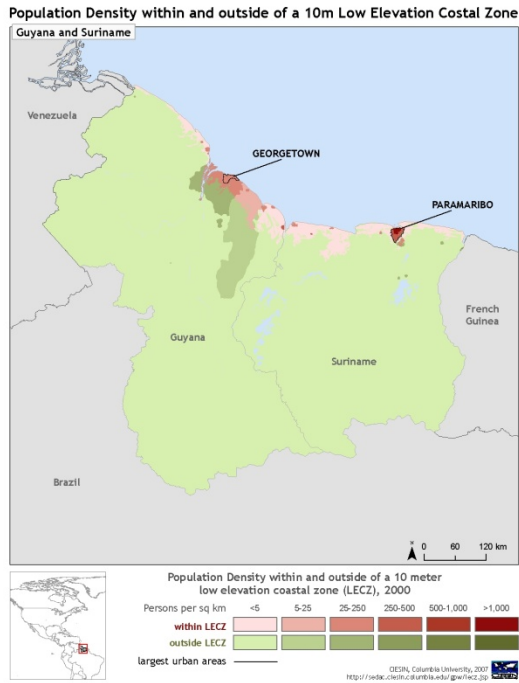
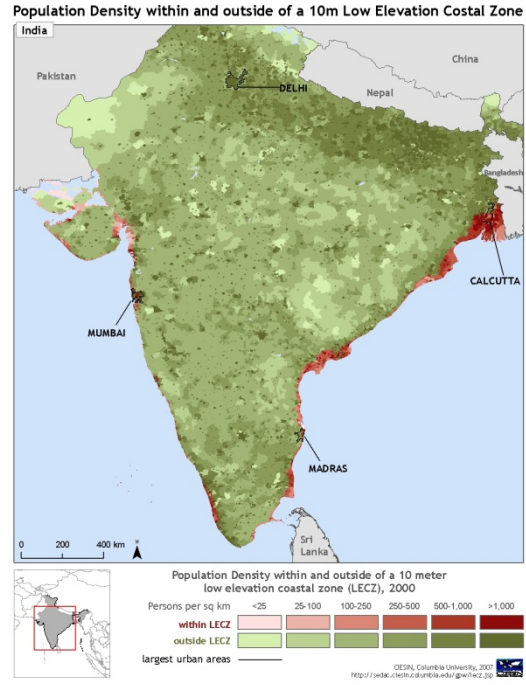
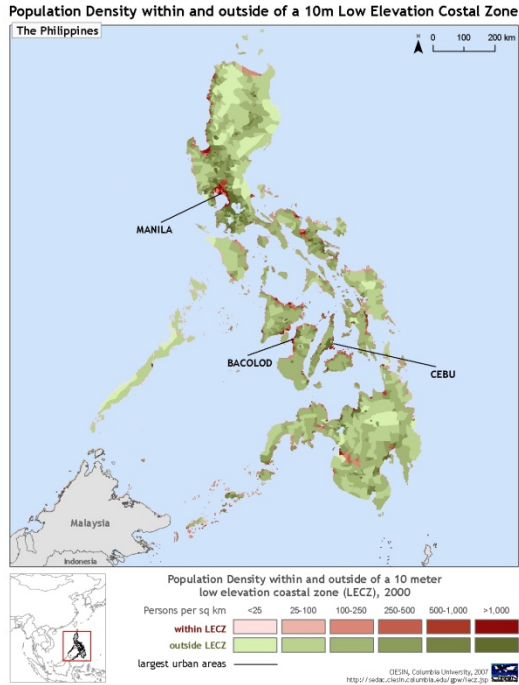


Almost all of Djibouti's population lives in the capital city, which is largely within the 10-meter LECZ. As a result, 41% of the country's population is within the LECZ.

Population Density within and outside of a 10m Low Elevation Coastal Zone

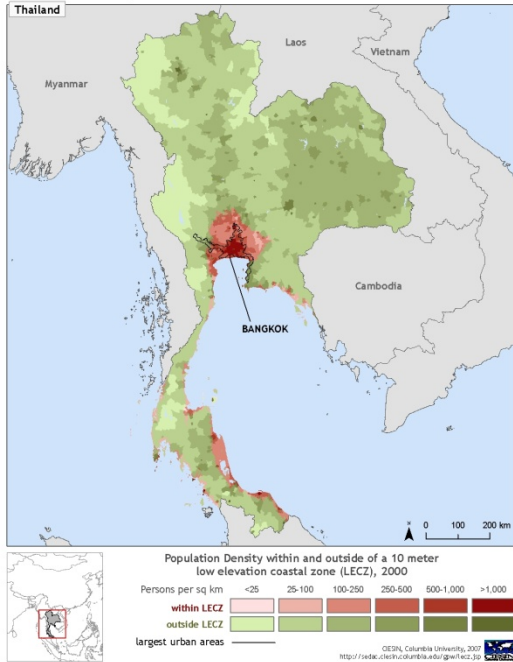


There are dense population centers throughout the Netherlands, but because so much of the country is at low elevations, 74% of the population lies within the 10-meter LECZ -- the 5th-highest value in the world.

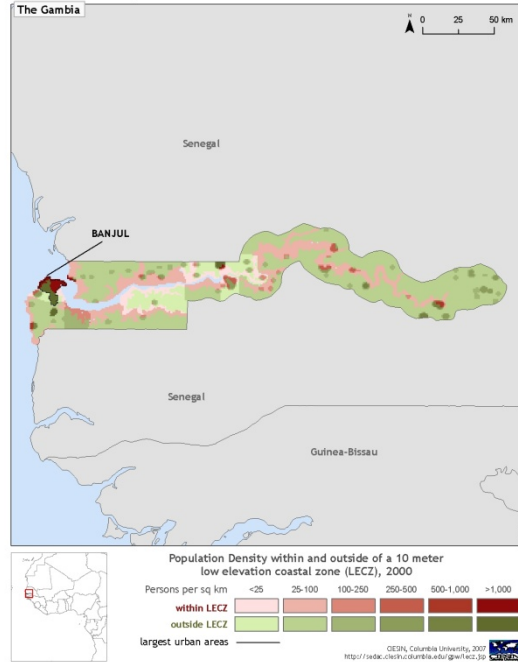


Assessment of Select Climate Change Impacts on US National Security

Population Density within and outside of a 10m Low Elevation Coastal Zone



Population Density within and outside of a 10m Low Elevation Coastal Zone



Module 2: Aggregate Impacts of Temperature Change

The Fourth Assessment of the IPCC, Working Group 2, contains an analysis of vulnerability to climate change at the country level (Yohe et al 2007)⁵ that takes into account projected temperature change and levels of adaptive capacity. The analysis utilizes methodologies elaborated in Yohe et al (2006b).⁶

The methodology relies on country-level estimates of changes in temperature associated with specific emission scenarios, over specified time frames, utilizing the software COSMIC to generate such estimates from an ensemble of general circulation model runs. COSMIC allows for selection of an assumed climate sensitivity of 1.5 or 5.5 degrees centigrade. Climate sensitivity is the temperature change associated with a doubling of CO₂ concentrations. The most recent IPCC report estimates that climate sensitivity is likely within the range of 2-4.5 degrees centigrade, but may be higher than 4.5; it is very unlikely to be less than 1.5. A number of studies estimate climate sensitivity to be above the IPCC bound. We selected the 5.5 degree option because it seemed more consistent with the general thrust of the IPCC report, though it should be noted that this is outside the IPCC's likely range. For the purpose of this study, in which we are identifying countries at relatively high risk as opposed to predicting the most likely future temperature, this is suitable.

Adaptive Capacity is measured as a function of a range of socioeconomic features including dependency ratios and literacy rates (Brenkert and Malone 2005)⁷. Country values for adaptive capacity are normalized to the global mean, so that values above 1 correspond to above-average capacity, and values less than 1 correspond to below-average capacity. An index of climate change vulnerability is calculated as the ratio of projected temperature change to normalized adaptive capacity. In effect, below-average capacity serves as a magnifier of temperature effects, while above-average capacity serves as a dampener.

A total of 36 separate scenarios were explored by Yohe et al (2006a)⁸, while 8 were explored in 2006b. The scenarios examined in these prior works were based on the A2 and B2 SRES emission scenarios. We utilized these two in our analysis, and added the A1

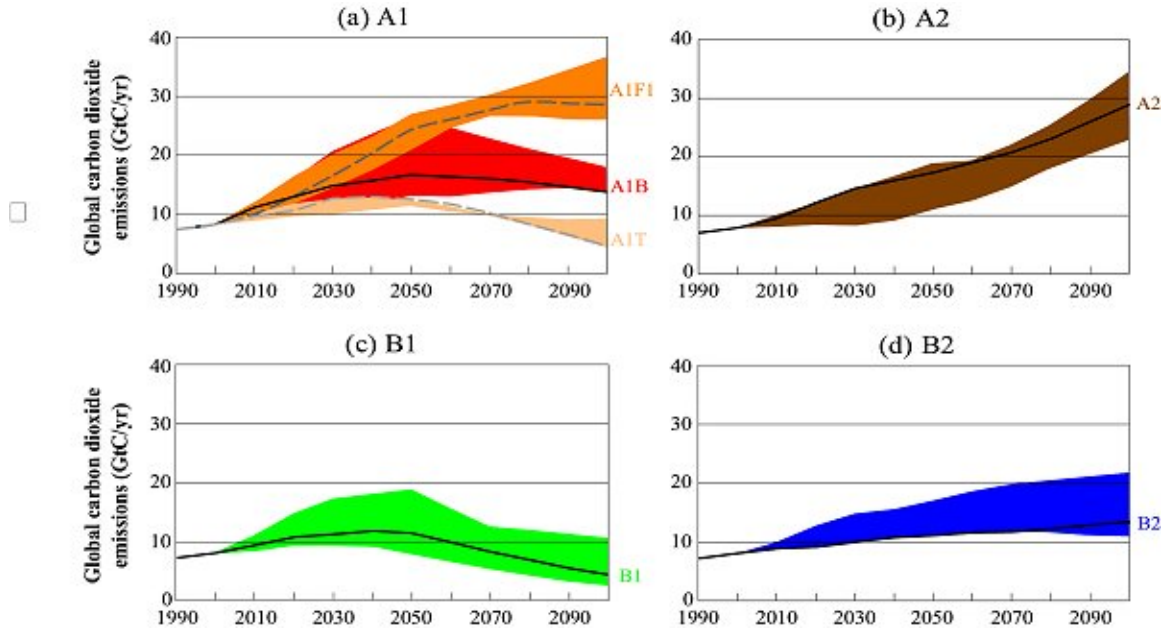
⁵ Gary W. Yohe and Rodol D. Lasco, Coordinating Lead Authors, IPCC WGII Fourth Assessment Report, Chapter 20: Perspectives on Climate Change and Sustainability, Final Draft for Government Review.

⁶ Gary Yohe et al, "Global Distributions of Vulnerability to Climate Change," *Integrated Assessment Journal* 6,3 (2006), 35-44. In its capacity as operator of the Socioeconomic Data Distribution Center for the IPCC (<http://sedac.ciesin.columbia.edu/ddc/>) and participation in the Task Group on Data and Scenario Support for Impact and Climate Analysis (TGICA), CIESIN assisted in the data compilation and mapping activities associated with this analysis. In addition CIESIN's Environmental Sustainability Index was used in some cases for imputation purposes.

⁷ Brenkert, A. and Malone, E., "Modeling Vulnerability and Resilience to Climate Change: A Case Study of India and Indian States," *Climatic Change* 72 (2005) 57-102.

⁸ Yohe, G., E. Malone, A. Brenkert, M. Schlesinger, H. Meij, X. Xing, and D. Lee. 2006. "A Synthetic Assessment of the Global Distribution of Vulnerability to Climate Change from the IPCC Perspective that Reflects Exposure and Adaptive Capacity." Palisades, New York: CIESIN (Center for International Earth Science Information Network), Columbia University. <http://ciesin.columbia.edu/data/climate/>.

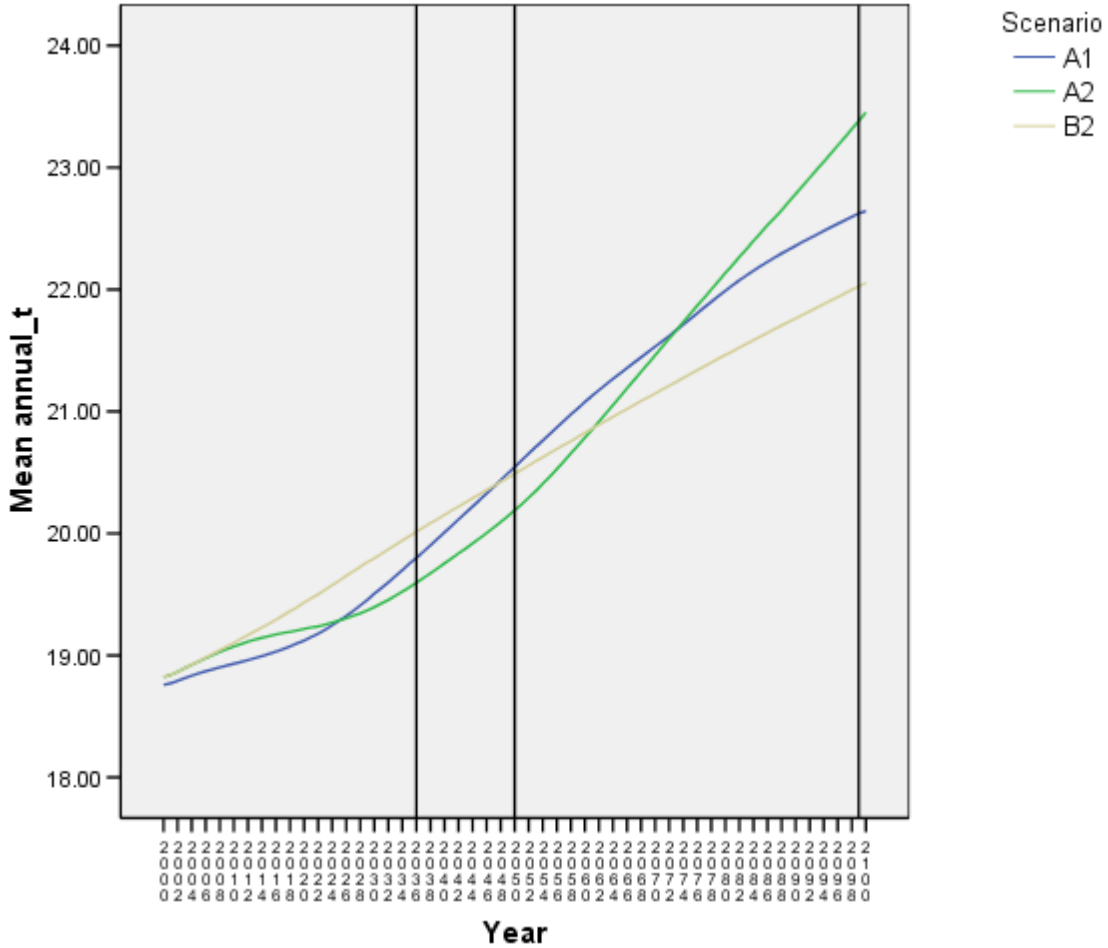
scenario. The A2 emission scenario is a high-emission scenario that is also characterized by low levels of economic growth in Africa through 2030. The B2 scenario is a lower-emission scenario characterized by more even global economic growth rates. A1 falls roughly in between the other two.



Comparison of Emission Scenarios.

Source: IPCC Special Report on Emissions Scenarios, Summary for Policy Makers, accessed online at <http://www.grida.no/climate/ipcc/emission/spm-3.htm>.

The rank-order of these scenarios varies over time, however.



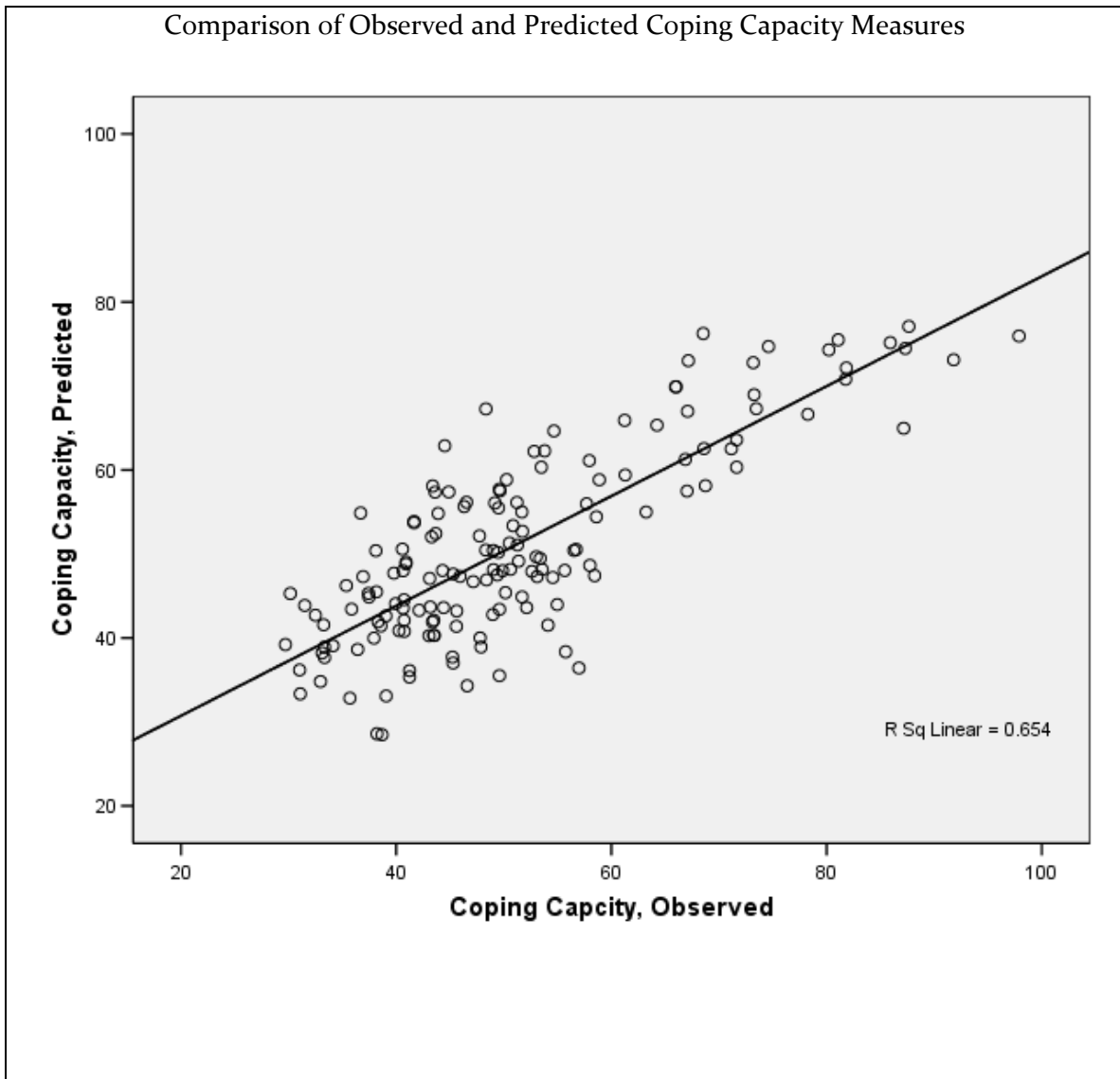
This graph shows annual temperature (degrees C), averaged over all countries and all 12 months, on a yearly basis. Reference lines are shown for 2030, 2050, and 2100. This demonstrates that which scenario is high, medium or low varies over time, and in fact the rank orders are different for each of these benchmark years.

The vulnerability scenarios explored by Yohe et al allow for adaptive capacity to either remain static or to increase over time, until it reaches the global mean or increases by 25%, whichever is largest. They also allow for the introduction of greenhouse gas mitigation to constrain carbon dioxide concentration in the atmosphere to 550 ppm. The scenarios that call for stabilization at 550 ppm are denoted by the suffix “S5.” The Yohe et al approach analyzes two end points, 2050 and 2100. In this study we focused on the year 2030.

The Yohe et al results had values for 110 countries. A large number were missing due to lack of adaptive capacity measures. Malone and Brenkert (2007)⁹ calculated adaptive capacity measures for an additional 50 countries. We imputed missing capacity measures

⁹ Elizabeth L. Malone and Antoinette L. Brenkert, “Vulnerability, Sensitivity, and Coping/Adaptive Capacity Worldwide,” chapter 3 in *The Distributional Effects of Climate Change: Social and Economic Implications*, forthcoming.

for 19 countries, using a multiple regression based on relevant indicators (World Bank governance indicators, commodity trade dependence, infant mortality, immunization rates, and male/female life expectancy ratio). We were therefore able to calculate a vulnerability index for 179 countries, using the Yohe et al methodology.



Countries with Imputed Adaptive Capacity Measures	
Country	Imputed Adaptive Capacity, as Fraction of World Mean
Antigua/Barbuda	1.13
Bahamas	1.33
Comoros	0.69
Dominica	1.01
Fiji	0.92
Iceland	1.51
Luxembourg	1.47
Maldives	1.04
Saint Lucia	1.03
Saint Vincent/Grenadines	1.01
Sao Tome/Principe	0.71
Seychelles	1.00
Singapore	1.59
Solomon Islands	0.74
Taiwan	1.22
Vanuatu	0.95
Western Samoa	1.00

To ensure consistency, we generated a set of country outputs from COSMIC for all 179 countries, for the period 2000-2100. We calculated benchmarks for years 2030, 2050 and 2100. For 2030 and 2050, we utilized a 3-year moving average of mean monthly temperature for the 3-year period centered around 2030 and 2050, respectively. For 2100, we utilized a 3-year average of mean monthly temperature for the period 2098-2100.

Because we generated COSMIC output ourselves and normalized by a new set of capacity measures, these results are not strictly comparable with those we presented in our April 2007 report. The rank orders are broadly similar; where they differ substantially it is due to changes in the capacity measure. Kenya, for example, which was one of the most vulnerable countries identified in the April report, has a much higher capacity score in the latest data set and therefore does not appear as such an extreme outlier in the present vulnerability scores.

Discussion of missing data

The following countries and territories lacked COSMIC output, and we therefore were unable to calculate a vulnerability index.

Countries and Territories Missing from Temperature-Change Vulnerability Analysis	
American Samoa	Martinique
Andorra	Mayotte
Anguilla	Monaco
Aruba	Montserrat
Bermuda	Nauru
British Virgin Islands	Netherland Antilles
Cayman Islands	New Caledonia
Cook Islands	Niue
Faeroe Islands	Norfolk Islands
Falkland Islands	Northern Mariana Islands
Federated State of Micronesia	Palau
French Guiana	Pitcairn
French Polynesia	Puerto Rico
Gibraltar	Reunion
Greenland	Saint Helena
Grenada	Saint Kitts and Nevis
Guadeloupe	Saint Pierre and Miquelon
Guam	San Marino
Guernsey	Svalbard and Jan Mayen
Holy See	Tokelau
Hong Kong	Tonga
Isle of Man	Turks and Caicos Islands
Jersey	Tuvalu
Kiribati	United States Virgin Islands
Liechtenstein	Wallis and Futuna
Macao	West Bank/ Gaza
Marshall Islands	

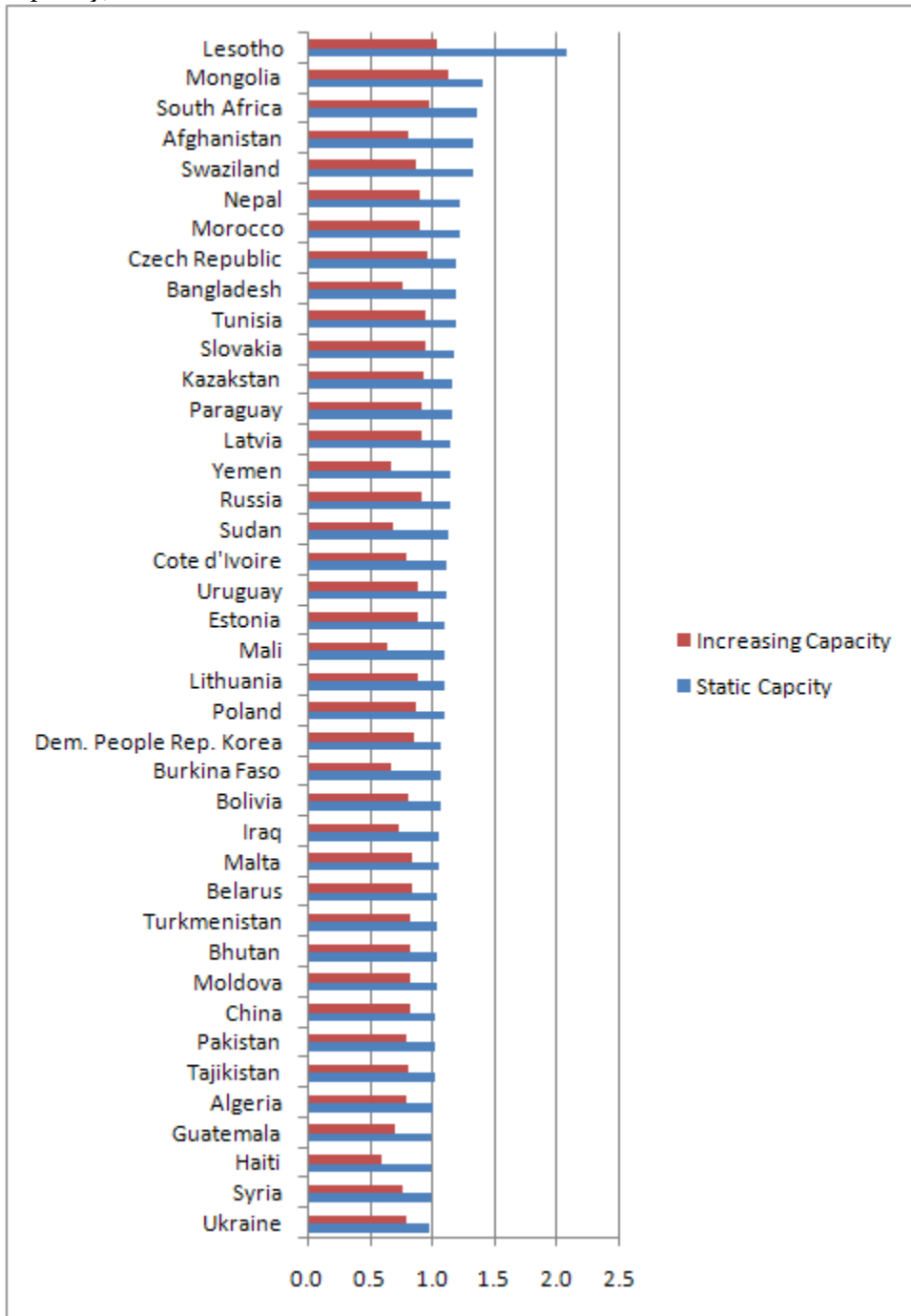
For the most part these are very small or micro states, which can probably be evaluated as a group for the purpose of assessing broad security linkages to climate change. The missing data point that is potentially the most problematic because of its potential security importance is that for the West Bank and Gaza. The omission here stems both from the fact that COSMIC’s algorithm for assigning grids to country borders was implemented prior to the implementation of the autonomy agreements, and that there is relatively little data available for estimating a quantitative coping capacity score. One could use the vulnerability score of Jordan as a rough proxy for the West Bank and Gaza, because it is nearby and has roughly similar coping capacity factors.

East Timor and Eritrea were not included in the COSMIC output or in the updated Coping Capacity measures. For the purpose of this analysis we assigned the Indonesia’s scores to East Timor and Ethiopia’s scores to Eritrea. They should be considered broadly illustrative but somewhat less precise than other country estimates.

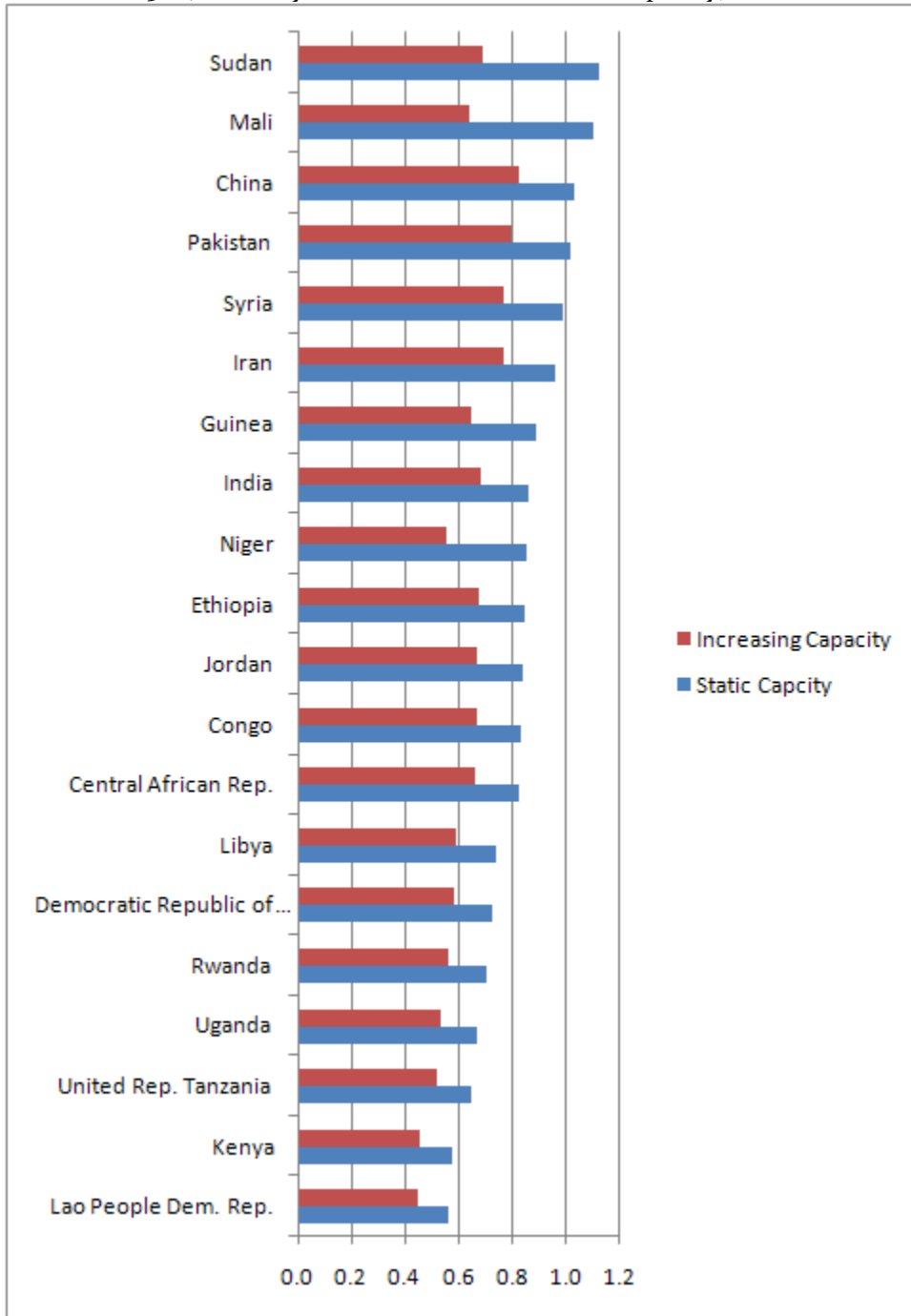
Results

These results are based on the A1 emission scenario for the sake of simplicity. Results for A2 and B2 are summarized at the end for purpose of comparison. Because B2 is a very low-emission scenario, it generates low levels of temperature change and therefore the scores are most very different from A2 and B2. Within each graph, values are shown representing the score that assumes no change in current levels of adaptive capacity, and scores that allow for capacity levels to increase. We show results for 2030, although we have calculated them for 2050 and 2100 as well.

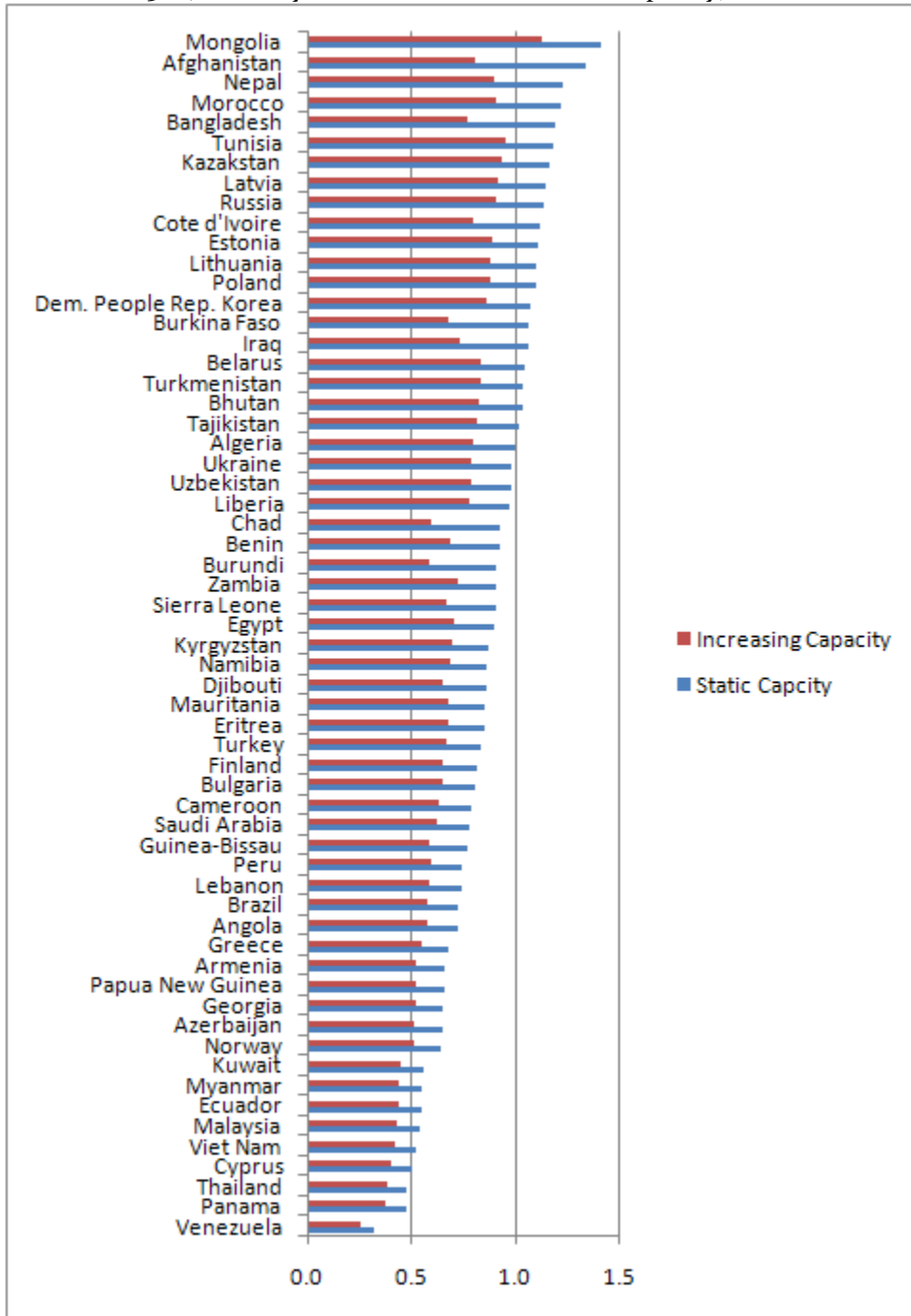
Top-40 countries with highest aggregate vulnerability to climate change scores, as projected in year 2030 under emission scenario A1 (sorted by scores that assume static capacity).



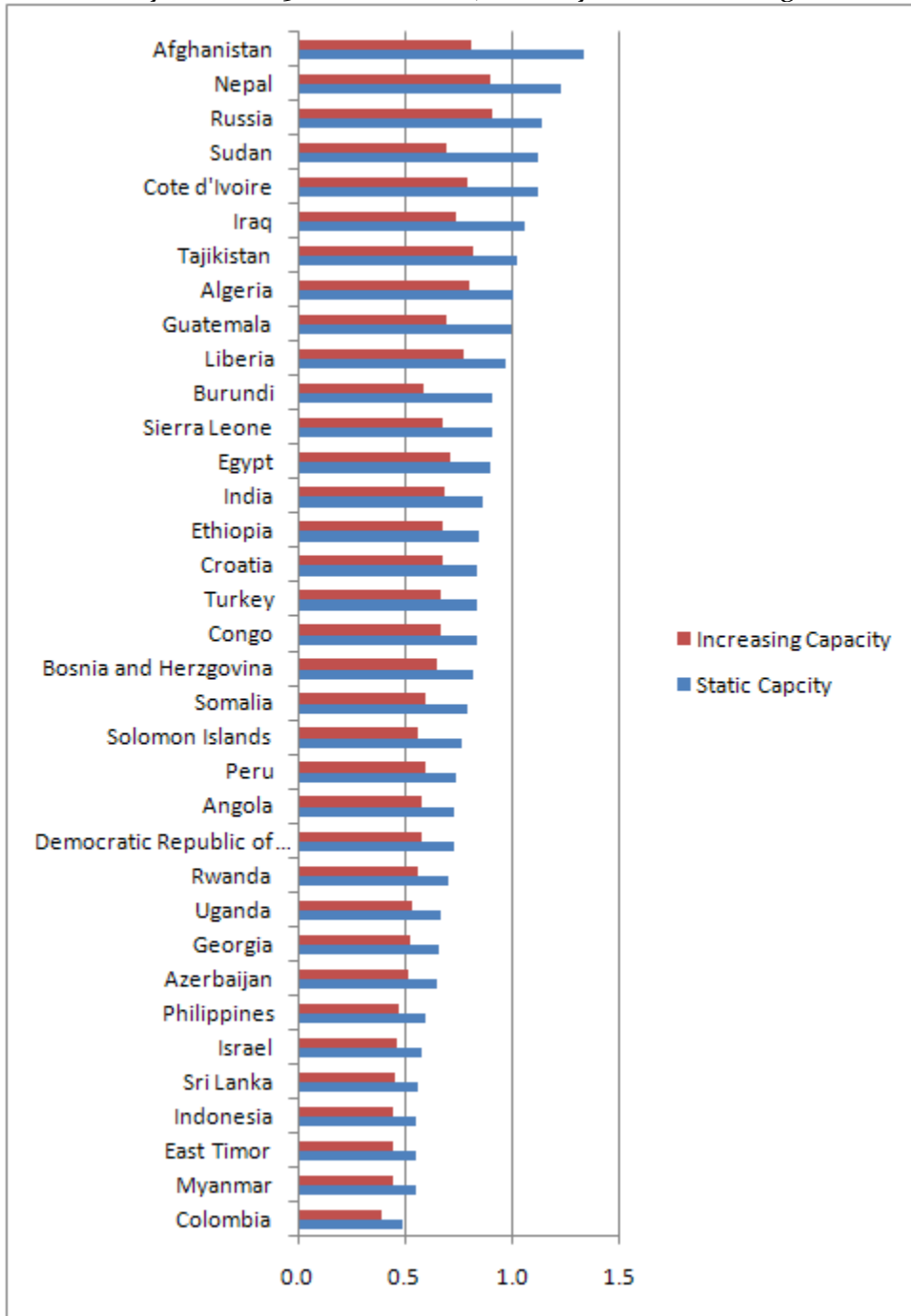
Countries in extremely dangerous neighborhoods, climate vulnerability scores, A1 scenario, 2030 (sorted by scores that assume static capacity)



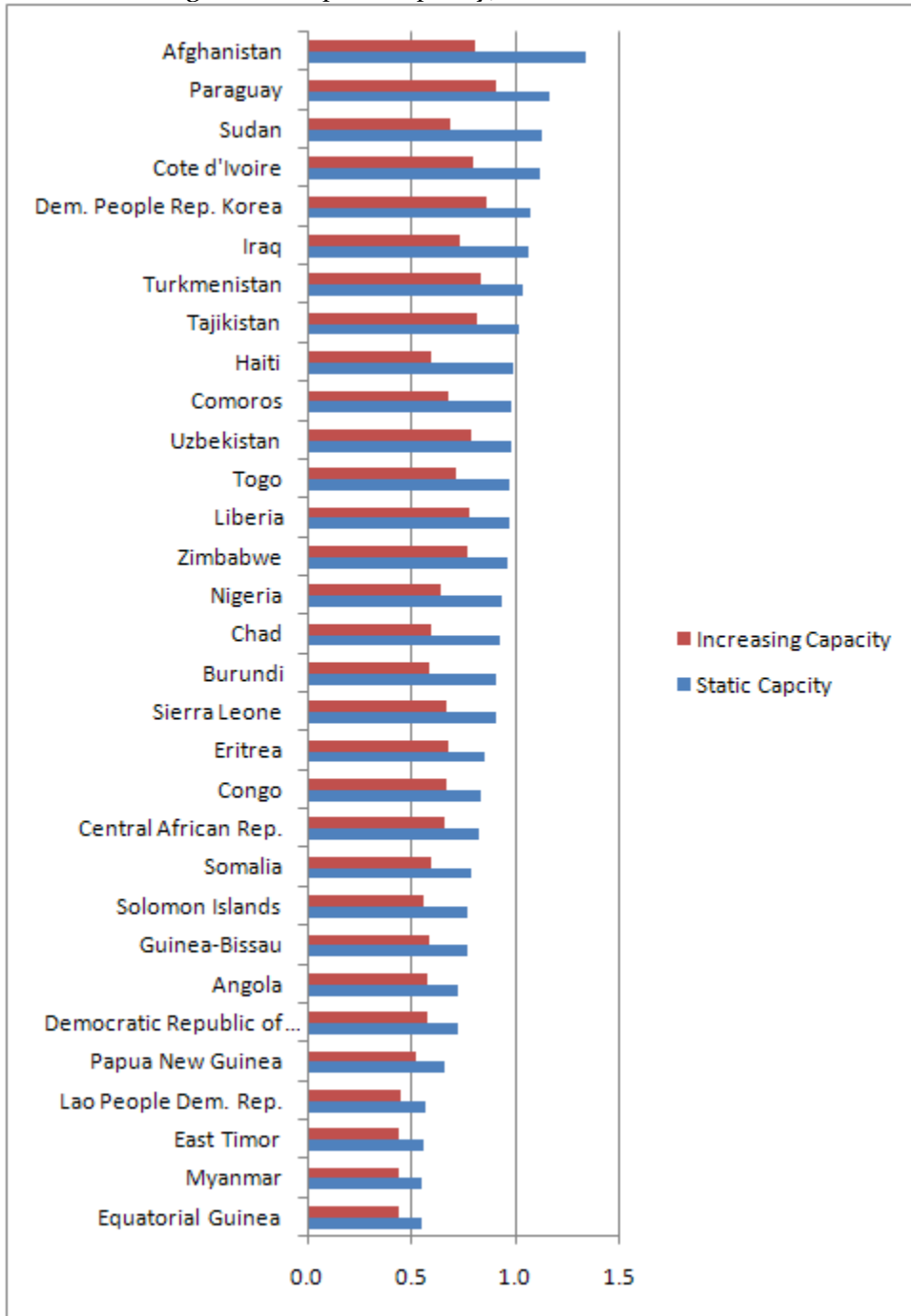
Countries in moderately dangerous neighborhoods, climate vulnerability scores, A1 scenario, 2030 (sorted by scores that assume static capacity)



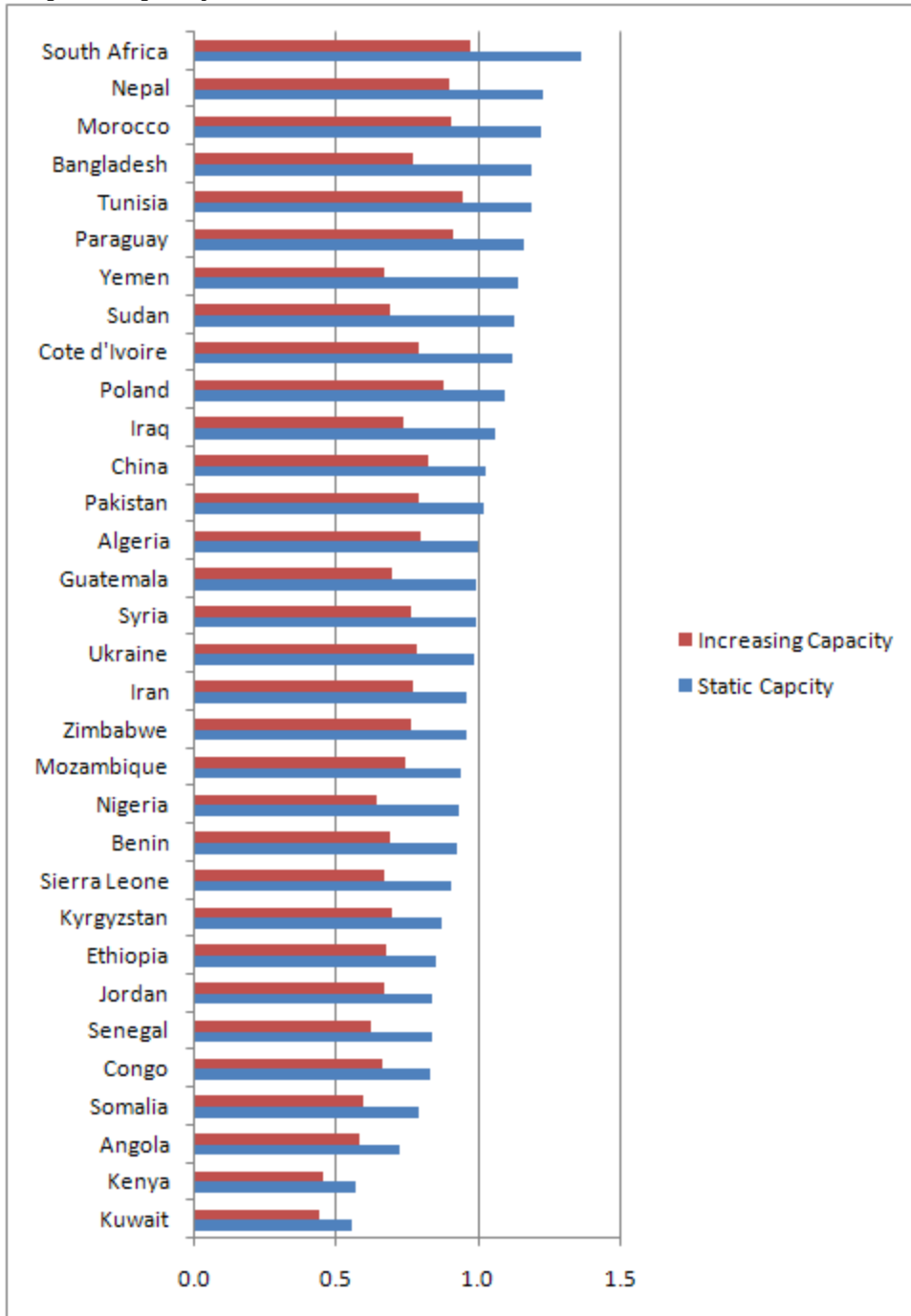
Countries with Extremely or Moderately High Crisis History 1990-20005, Climate Vulnerability Scores 2030, A1 scenario (sorted by scores assuming static adaptive capacity)



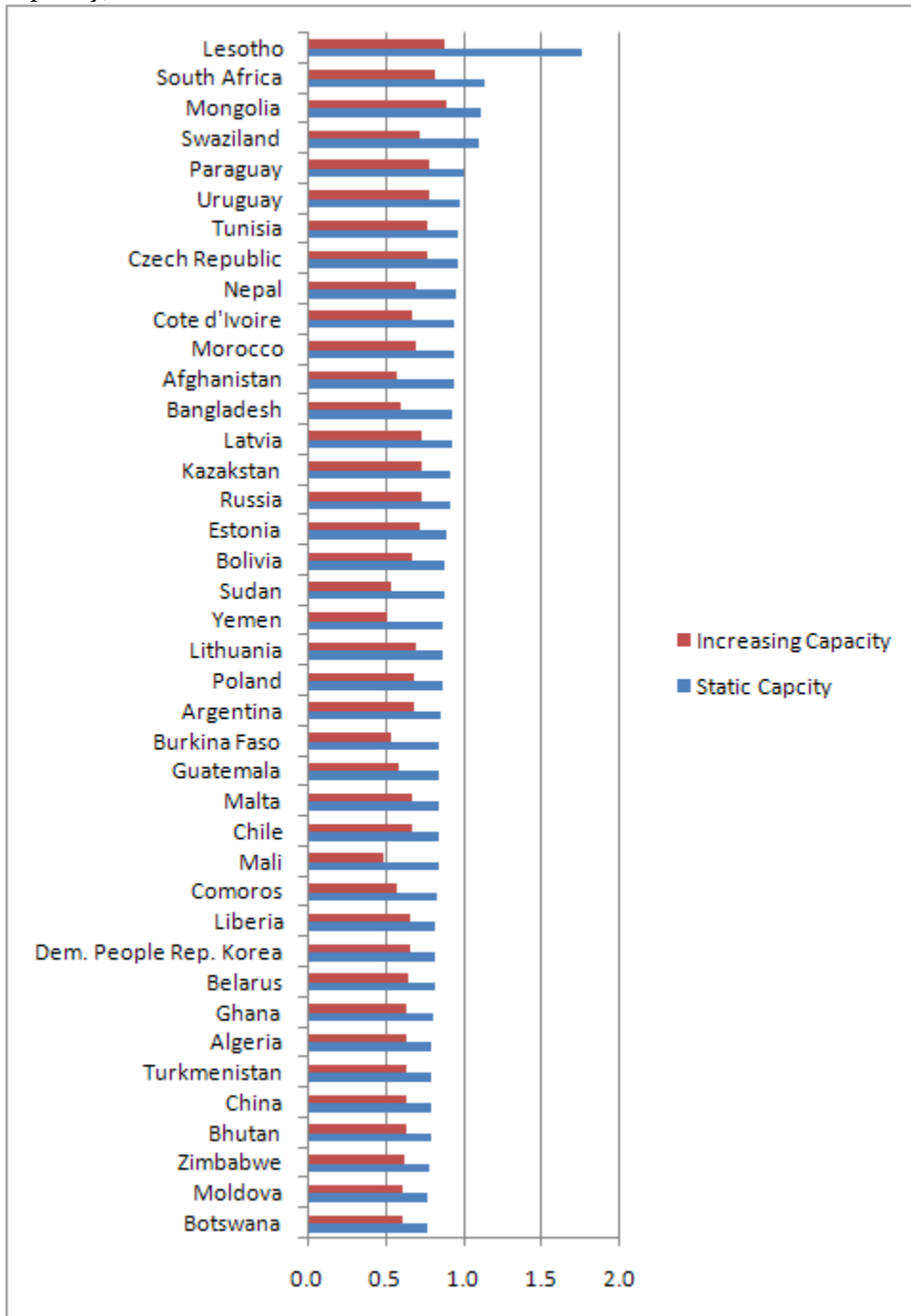
Countries with very low capacity, climate vulnerability scores 2030, A1 scenario (sorted by scores assuming static adaptive capacity)



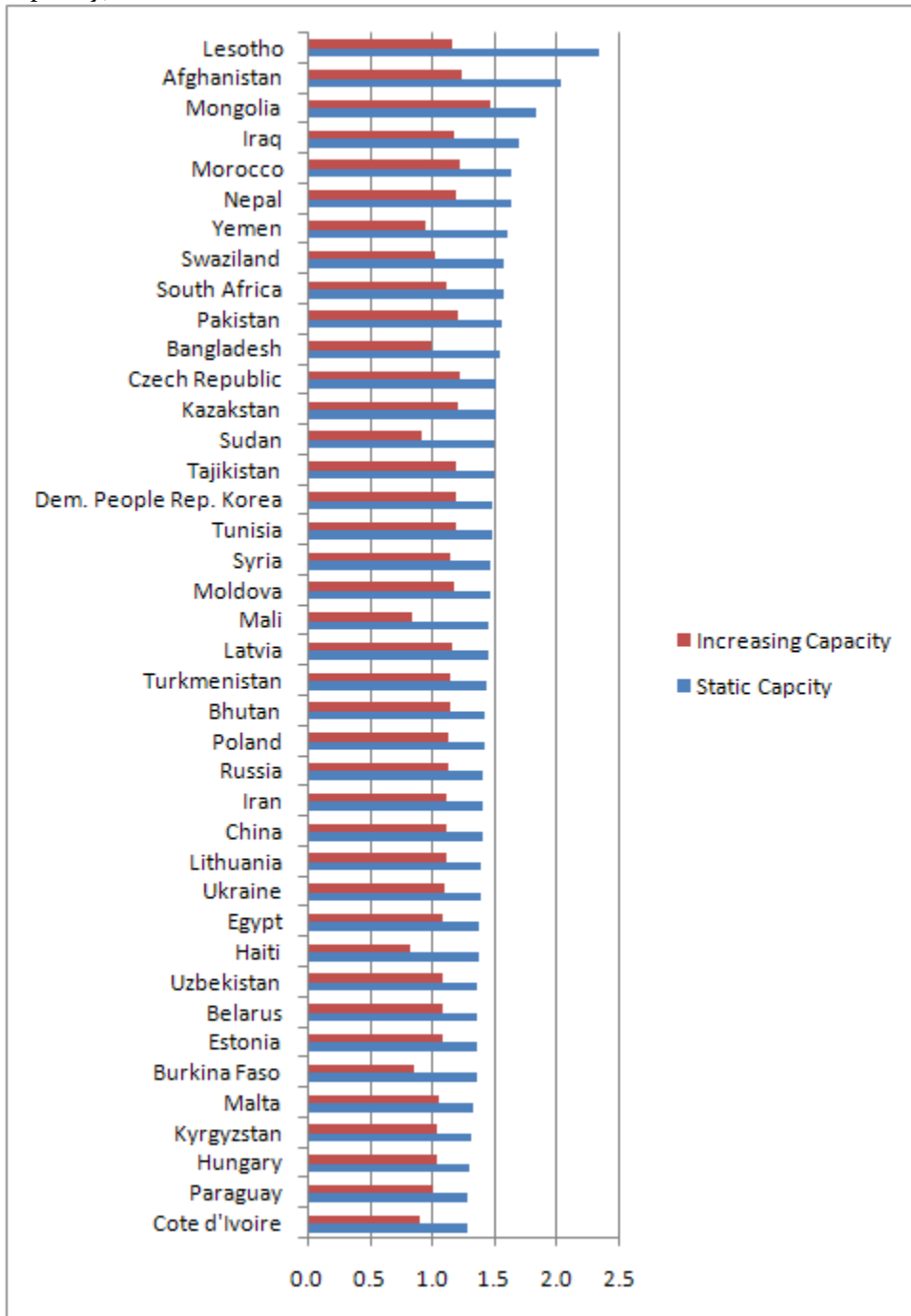
Countries with two or more risk factors (low capacity, high crisis history, dangerous neighborhood), climate vulnerability 2030, A1 Scenario (sorted by score assuming static adaptive capacity)



Top-40 countries with highest aggregate vulnerability to climate change scores, as projected in year 2030 under emission scenario A2 (sorted by scores that assume static capacity).



Top-40 countries with highest aggregate vulnerability to climate change scores, as projected in year 2030 under emission scenario B2 (sorted by scores that assume static capacity).



Module 3: Water Scarcity

Hydrology Projections:

To explicitly account for the human interventions in the water cycle in a modeling framework, we used a recently modified version of the Water Balance Model (WBM) (Vörösmarty et al. 1998), the WBMPlus model. The modifications include a reservoir routing module that simulates the operation of large reservoir and its impacts on river discharge and an irrigation module that models the interactions of irrigated areas with components of the hydrological cycle. The WBMPlus model is a physically based, grid-cell based macroscale hydrological model that simulates variations of components of the hydrological cycle based on physical datasets.

To simulate contemporary and future hydrology conditions climate change fields were acquired from the World Climate Research Programme's (WCRP's) Coupled Model Intercomparison Project phase 3 (CMIP3) multi-model data holdings (Meehl, et al., 2007, http://www-pcmdi.llnl.gov/ipcc/about_ipcc.php) and used as input into the WBMPlus model. The WCRP CMIP3 data holdings represent a coordinate set of global coupled climate model runs from the IPCC Fourth Assessment Report (AR4). A global monthly time series and long term means for contemporary (1986–2015) and future (2016 – 2045) runoff and river discharge were computed with the WBMPlus model using off-line atmospheric forcings from the CMIP3 ECHAM5 scenario datasets. The contemporary state was simulated using the ECHAM5 20C3M twentieth-century simulation model input to year 2000 with anthropogenic and natural forcings for time period 1986-2015. The future state for year 2030 was simulated using the ECHAM5 twenty-first-century climate change simulation with SRES A1B (medium forcing, i.e., CO₂ concentration of about 700 ppm by 2100) for time period 2016-2045. Long term mean runoff fields from the WBMPlus runs were constrained by observed discharge monitoring data and converted to discharge by integrating along a digitized river network (Fekete et al., 1999, Vörösmarty, et al., 2000a). Results from the ECHAM5 20C3M and SRESA1B scenarios were used to predict incremental differences between contemporary and future runoff and discharge for individual grid cells.

Population Projections:

A globally distributed geography of contemporary population for year 2000 was developed from a 1-km data set (Vörösmarty, et al. 2000b) aggregated to the 30-minute grid cell resolution. Future population distribution for year 2030 was calculated using a cumulative growth rate surface derived from the IIASA estimates of population (Grubler et al, 2006). The growth rate was applied to the contemporary population dataset at 30-minute resolution to create future estimate. The contemporary and future population datasets were used in conjunction with modeled hydrology outputs to estimate water scarcity and water crowding for present and future conditions.

Water Crowding/Water Scarcity Index

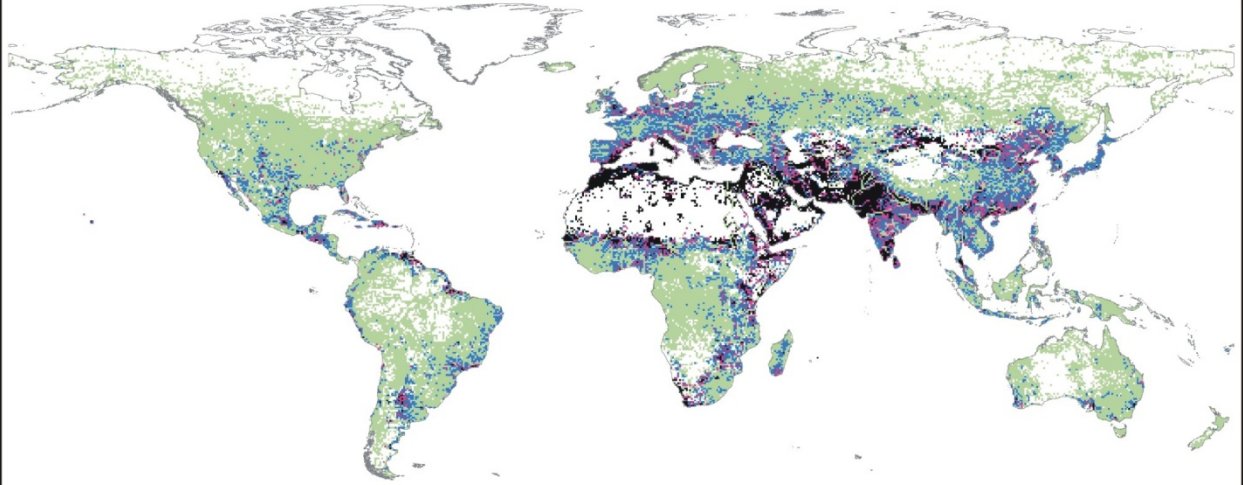
A water crowding and water scarcity index was adapted from Falkenmark and Lannerstad (2005) as indicators of the impacts of climate and population change on sustainable water resources. Both the water crowding and water scarcity index reflect the relationship between the available water supply and the number of people that can be supported in a

sustainable way taking into account food security, household use, and industry and energy production. The water crowding and water scarcity indices are reciprocal measures both describing the relationship between water availability and the number of people that can be sustainably supported by that water supply. The water crowding index is expressed in terms of the number of people supported by a water flow unit of 1 million cubic meters per year in a given area. The water scarcity index is expressed as the amount of water available per person in a given area.

Thresholds of water crowding and water scarcity have been defined to describe the different levels of water stress and potential levels of need. An absolute “water barrier” for sustainable use has been defined as $< 500 \text{ m}^3/\text{person}$ (water scarcity) or > 2000 people/flow unit (water crowding). Below this barrier available water supplies are insufficient to meet the needs of the population and alternative and often costly means to increase water supply must be considered, often incurring financial and human welfare burdens. Between $500 \text{ m}^3/\text{person}$ and $1700 \text{ m}^3/\text{person}$ water scarcity (or $600 - 2000$ people/flow unit water crowding) populations are defined as being under “water stress” conditions. Within this threshold available water supplies are strained by water needs. This threshold serves as a warning sign to places expected to experience population growth, increases in future water demand for agriculture or industry and vulnerability to potential impacts of climate change. We have defined people falling in the $1700 - 5000 \text{ m}^3/\text{person}$ water scarcity (or $100 - 600$ people/flow unit water crowding) range as populations vulnerable to water stress. Given unchecked future changes in population, agricultural/industrial demand and/or climate change these areas could be vulnerable to water stress conditions in the future.




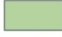

Against the contemporary year 2000 benchmark we formulated three scenarios to quantify the contributions of climate change and development pressure to the degree of relative water stress in 2030. The “Climate Only” scenario varied climate and subsequent modeled discharge for year 2030 but fixed the magnitude and spatial distribution of human population at year 2000 levels. The “Population Only” scenario applied projected population growth for year 2030 but used discharge based on the contemporary climate. The “Climate and Population Change” scenario changed both climate and population growth for year 2030.

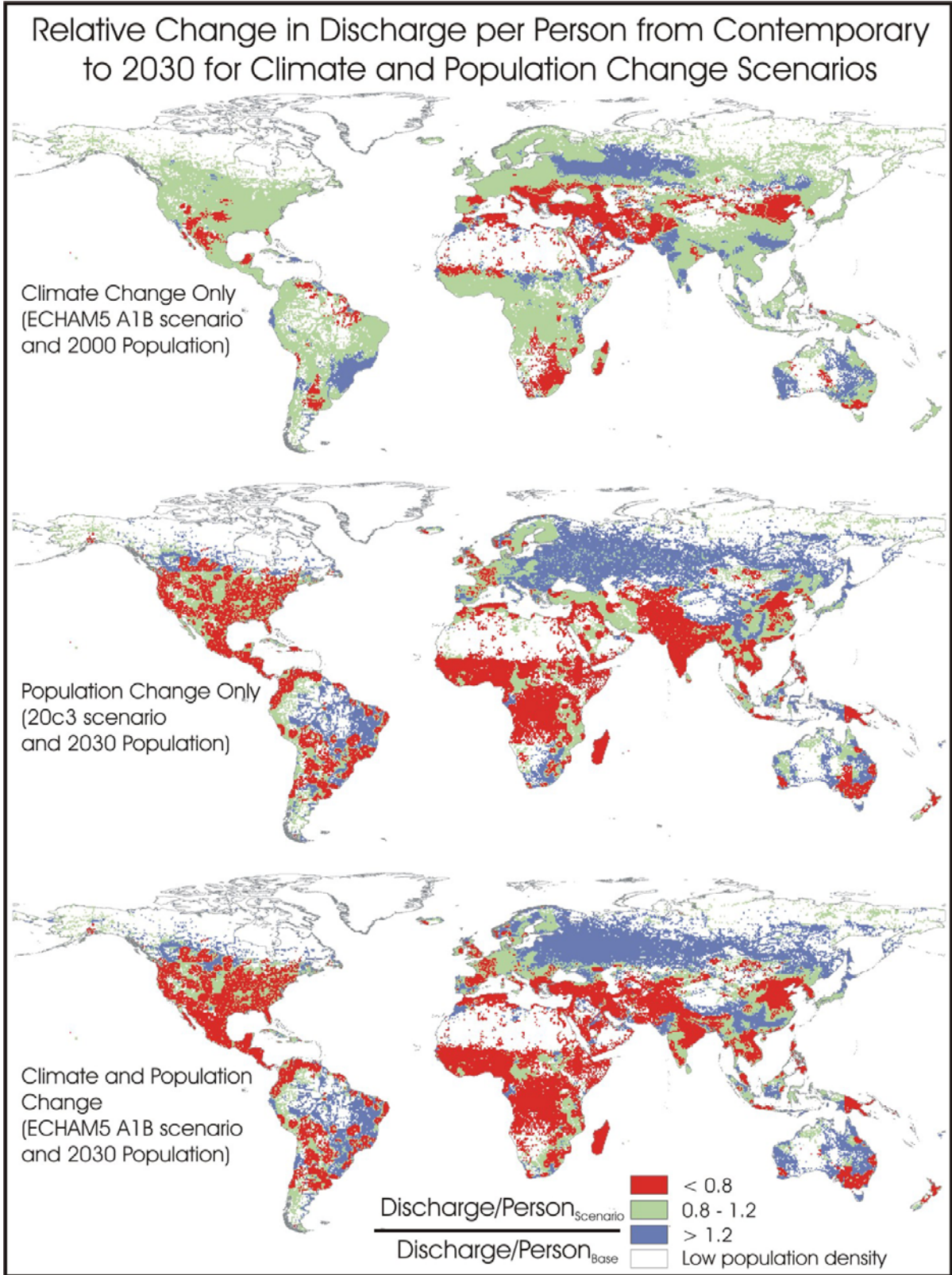
Water Scarcity Index for Contemporary Conditions

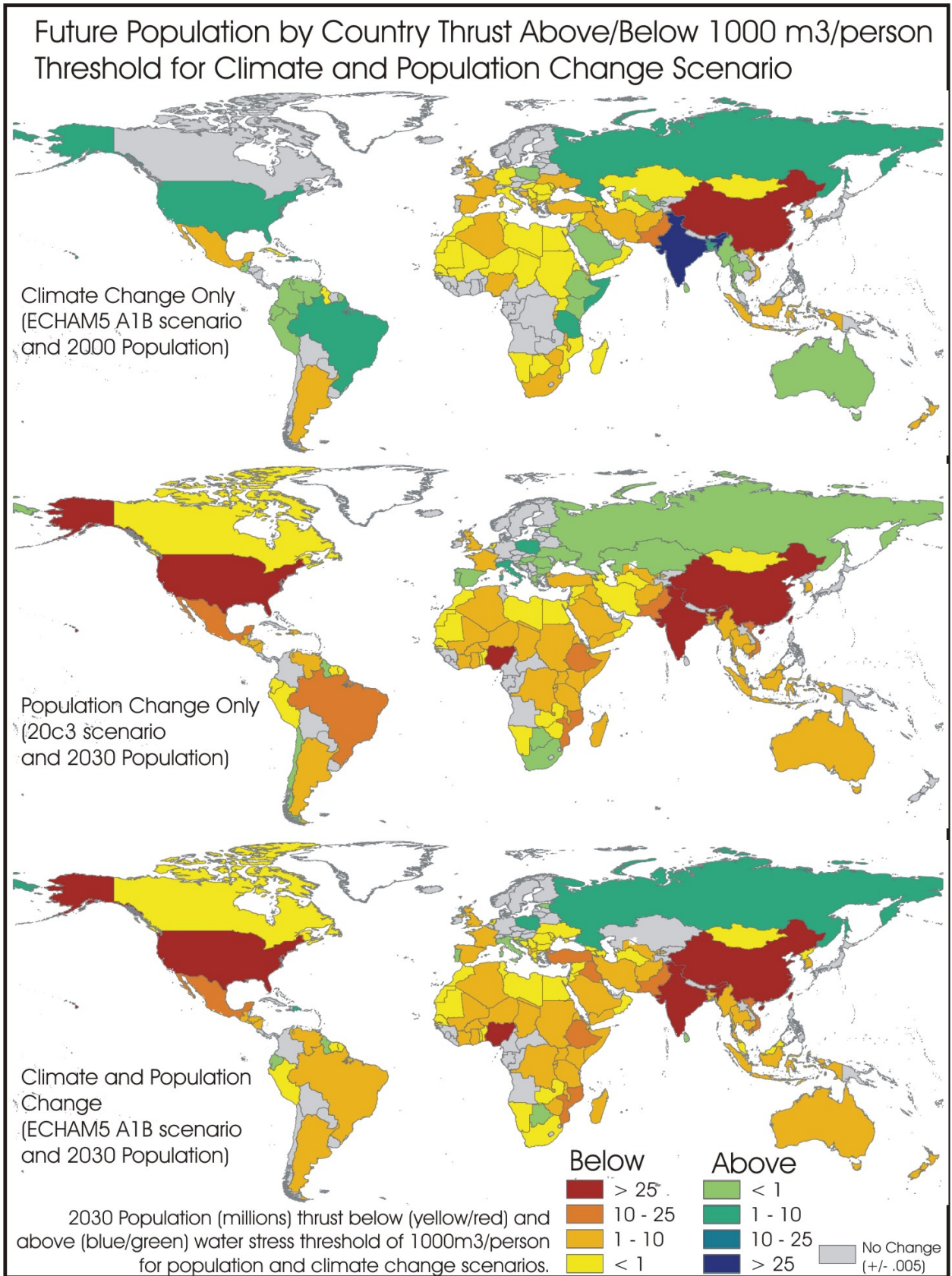


The water scarcity index describes the relationship between water availability and the number of people that can be supported by that water supply. The scarcity index is expressed in terms of the number of people per flow unit where a flow unit of water is equal to 1 million cubic meters per year.

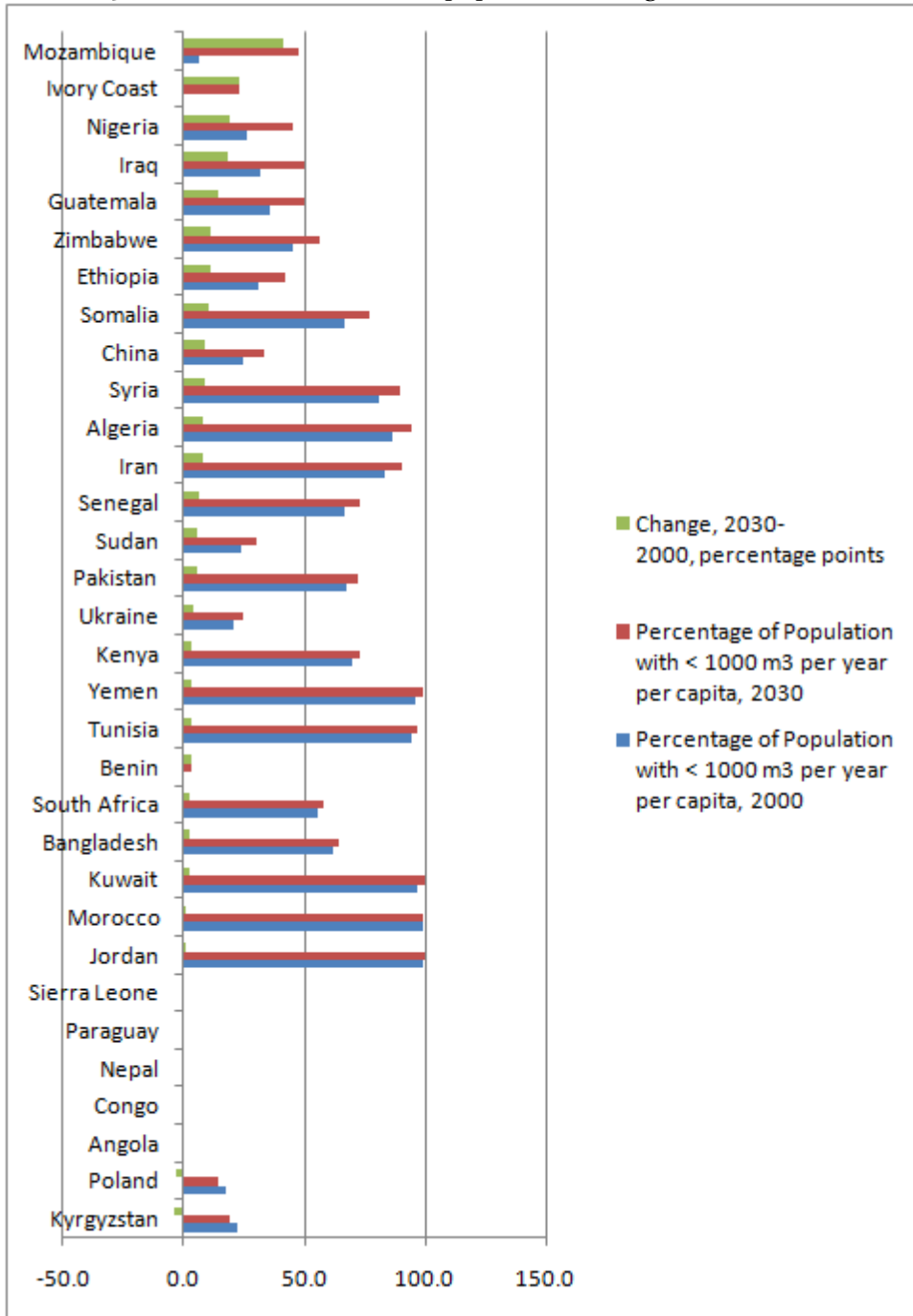
Water Scarcity Index

-  Water Barrier (> 2000 people/flow unit)
-  Water Scarcity/Stress (600 - 2000 people/flow unit)
-  Populations Vulnerable to Water Stress (100 - 600 people/flow unit)
-  Adequate Supply (< 100 people/flow unit)
-  Low Density Population





Countries with Two or More Instability Risk Factors (Dangerous Neighborhood, Crisis History, Low Capacity), Sorted by Change in Percentage of Population in Water Scarcity (2000-2030). Based on climate-and-population change scenario.



References

Fekete, B.M, *et al.*, *Global, Composite Runoff Fields Based on Observed River Discharge and Simulated Water Balances, Report 22* (World Meteorological Organization-Global Runoff Data Center, Koblenz, Germany, 1999).

Falkenmark, M. and Lannerstad, M. 2005. Consumptive Water Use to Feed Humanity – Curing a Blind Spot. *Hydrology and Earth System Sciences*, Vol. 9, Issue 1/2, pp.15-28.

Grubler, A., *et al.* (2006), Regional, national, and spatially explicit scenarios of demographic and economic change based on SRES, *Technological Forecasting & Social Change*, 74, 980-1029.

Meehl, G.A., C. Covey, T. Delworth, M. Latif, B. McAvaney, J.F.B. Mitchell, R.J. Stouffer, and K.E. Taylor, 2007: THE WCRP CMIP3 Multimodel Dataset: A New Era in Climate Change Research. *Bull. Amer. Meteor. Soc.*, 88, 1383-1394.

Vörösmarty, C.J., Federer, C.A. & Schloss, A.L. (1998), Potential Evaporation functions compared on US watersheds: Implications for global-scale water balance and terrestrial ecosystem modeling, *Journal of Hydrology* 207, 147-169.

Vorosmarty, C. J., B. M. Fekete, M. Meybeck and R. B. Lammers (2000), A Simulated Topological Network Representing the Global System of Rivers at 30-Minute Spatial Resolution (STN-30) , *Global Biogeochem. Cycles*, 14, 599 - 621.

Vörösmarty, C.J., Green, P.A., Salisbury, J., & Lammers. R.B. (2000), Global water Resources: Vulnerability from Climate Change and Population Growth, *Science*, Vol 289, 284-288.